Remote Sensing in Earth Systems Sciences
https://doi.org/10.1007/s41976-019-00025-7

ORIGINAL PAPER

A Review of Satellite-Derived Soil Moisture and Its Usage for Flood Estimation

Seokhyeon Kim [1] · Runze Zhang [1,2] · Hung Pham [1,3] · Ashish Sharma [1]

Received: 28 October 2018 / Revised: 13 September 2019 / Accepted: 26 September 2019

Abstract
Accurate knowledge of the spatiotemporal behavior of soil moisture (SM) can greatly improve hydrological forecasting capability. While ground-based SM measurements exhibit greater accuracy, they tend to be sparse in space and available for limited periods. To overcome this, a viable alternative is space-borne microwave remote sensing because of the near real-time observational capability at the global scale. However, its direct applications have been limited because of the uncertainty associated and the coarse spatial resolution the products are available at. Considering its usefulness and limitations, this paper is intended to provide an extensive review of satellite-derived SM and its applications for assessing flood risk in sparsely gauged or ungauged catchments worldwide. Therefore, we aim to identify and discuss research gaps, and finally propose future research directions for improvement and hydrological applications of these SM products. The paper starts with a brief introduction to satellite-derived SM products and consists of three interdependent focal areas: evaluation, improvement, and application of the satellite SM for flood risk alleviation.

Keywords Flood · Soil moisture · Satellite remote sensing · Ungauged basins · Microwave · Improvements · Spatial disaggregation

1 Introduction

Water, the most plentiful material on Earth, is a necessity for all living things as well as a key to human existence and progress [24]. The water cycle, representing the continuous circulation of different phases of water without beginning or end, is important in the Earth system. Through the cycle, water vapor is evaporated from land/sea surfaces and condensed into clouds in the atmosphere. The water returns to the surface as precipitation and flows as runoff, infiltrates into the ground, or remains on the surface as water or snow. In the water cycle, significant anomalies (i.e., floods) have profoundly affected human survival and prosperity. Floods are frequent and devastating natural disasters which lead to significant loss of human lives and economic damage, with global average damage amounting to hundreds of millions of dollars per event [67]. In this regard, flood estimation has played an important role in mitigating the adverse impacts by ensuring that sufficient time is available for evacuation and where possible preventing socioeconomic damages [17]. Soil moisture (i.e., antecedent condition) and rainfall (i.e., external forcing) are critical elements that influence flooding in a watershed, and the combined effect of the spatiotemporal dynamics of soil moisture (SM) and rainfall can explain most of the variability in runoff prediction [52]. Therefore, flood estimation using traditional hydrologic models requires information on rainfall and SM in space and time [31].

This paper focuses on surface SM, which is defined here as the volumetric amount of water in the uppermost soil layer, as a key contributor to flooding, along with being a variable for which limited in situ observations are possible, creating an opportunity for satellite remote sensing approaches to fill in the gap. SM has persistence, also called "memory" [88], which directly interacts with precipitation, evaporation, and runoff [41]. Accordingly, it is well known

✉ Seokhyeon Kim
seokhyeon.kim@unsw.edu.au

[1] School of Civil and Environmental Engineering, University of New South Wales, Sydney, NSW 2052, Australia

[2] Present address: School of Engineering Systems and Environment, University of Virginia, Charlottesville, VA 22904, USA

[3] The University of Danang, University of Science and Technology, 54 Nguyen Luong Bang, Da Nang, Vietnam

Published online: 13 November 2019

that SM is a key driver of flooding in a watershed along with incident rainfall and topography [119, 176]. In this context, accurate knowledge of the spatiotemporal behavior of SM can improve the skill of hydrological forecasting [6, 15, 72, 84]. This is in line with existing studies on this topic, stating that antecedent SM affects runoff from medium- and low-intensity storms in semi-arid watersheds [18, 131] and flood events from heavy rain under humid climates [149]. Accordingly, the availability of SM at appropriate spatial and temporal resolutions is important in formulating effective forecasting systems [34, 144, 173].

While ground-based measurements have been a source of SM information, SM observations at large spatial scales have been significantly limited due to spatiotemporally heterogeneous nature of SM resulting from diverse climate, weather, topography, vegetation, land cover/land use, and soil type [29, 57]. Therefore, many parts of the world remain ungauged, with even those that are gauged generally poor in spatial distribution with limited temporal periods [45], especially in remote parts of the world. Over the past 20 years (1996–2015), more than 150,000 people have died from flooding, and more than 80% of them occur in low- or middle-income countries [25]. This disparity in global flooding death rates results from vulnerable geophysical locations and socioeconomic factors. Thus, improved flood estimation is greatly needed in low- and middle-income countries [2], where, in general, the hydrological monitoring and data acquisition tend to be poorer than in developed countries.

A viable alternative to ground measurements is microwave remote sensing using space-borne passive observations [36, 75], active microwave observations [171], or a combination [55]. Estimating surface SM using microwaves is based on a large contrast in dielectric constants of dry and wet soil [151]. Added to this, passive microwave is almost unaffected by cloud or rain at low frequency, with day and night observations; is less sensitive to surface roughness ([179]); and can provide information about the moisture content of the topsoil layer even under vegetation coverage [117]. Accordingly, these observations have provided a unique ability for retrieving SM in near real-time at global scales [37, 137], and the surface SM information has been widely used for various studies related to climate [11, 88, 107], flood [81, 104, 143], and drought [54, 63, 155]. An excellent review of how satellite remote sensing can assist in closing the catchment water balance is provided in Lakshmi et al. [91].

However, despite the potential capability of the satellite-derived SM for flood estimation, direct use has been limited due to the uncertainty resulting from various factors and/or the coarse spatial resolution products are available at [44, 86, 168]. Considering the usefulness and the limitations, the objective of this paper is to present a comprehensive review of satellite-derived SM and its applications for flood estimation. Accordingly, we aim to identify and discuss research gaps, and finally suggest future research directions toward improvements and hydrological applications of such SM products. For this purpose, in Section 2, we provide a brief background of satellite-derived SM. This includes a four-decade chronology of various passive and active microwave sensors which can be used for retrieving SM. Then we present an introduction to two types of retrieval algorithms using the passive and active sensors, where we discuss their differences and physical rationales referring to relevant studies. Then we cover research topics on various techniques for validating the SM products (Section 3), which are classified into traditional and advanced approaches. This article first presents the traditional approach using ground measurements in truth and discusses the limitations due to systematic differences between SM products and ground measurements. Next, we show recent advances to overcome the limitations of the traditional verification approaches and review the limitations that can be improved. In Section 4, we briefly introduce various statistical, mathematical, and physical methods addressing drawbacks in accuracy and spatial resolution of the SM products. Next, in Section 5, we discuss how the SM products have been used for flood estimation, based on a summary of relevant studies, including model calibration, data assimilation, rainfall correction, and flood monitoring. Then future studies were proposed based on the room for improvement identified through the reviewed literature. Finally, in Section 6, we present an integrated pathway for producing an improved SM product, which can provide enhanced flood forecasting capacity.

2 Satellite-Derived Soil Moisture Products

2.1 A Four-Decade Chronology

During the last four decades, satellite microwave remote sensing has become a unique tool for measuring surface SM at global scales. Currently, as shown in Fig. 1, microwave observations have long-term availability and diversity. The first passive microwave observations resulted from the Scanning Multichannel Microwave Radiometer (SMMR) onboard the Nimbus-7 satellite in 1978, observing brightness temperatures through multiple channels including C-band (6.6 GHz) used for SM retrieval. Data has now been available using several active/passive sensors over the past four decades (Fig. 1). The L-band has been used for Soil Moisture and Ocean Salinity (SMOS), SAC-D (Spanish: Satélite de Aplicaciones Científicas-D for Satellite for Scientific Applications-D), and Soil Moisture Active Passive (SMAP), and the X- and C-bands have been used for others such as the Microwave Radiation Imager (MWRI) onboard FengYun-3B satellite and the Advanced Microwave Scanning Radiometer for the Earth Observing System (AMSR-E) and Advanced Microwave Scanning Radiometer 2 (AMSR2) mounted on

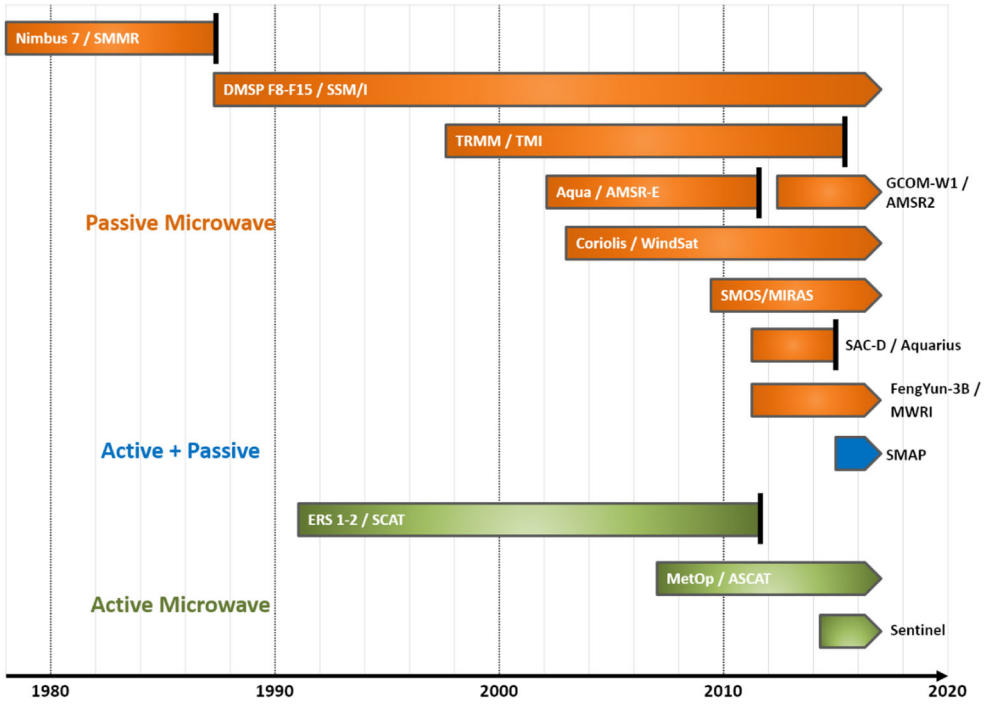

Fig. 1 Timeline of space-borne radiometers (passive microwave), scatterometers (active microwave), and a combination that can be used for retrieving surface soil moisture on global scales (updated from Dorigo et al. [44])

Aqua and GCOM-W1 satellites, respectively [10, 37, 55, 75, 128, 130].

The C-band (5.3 GHz) Scatterometer (SCAT) onboard European Remote Sensing (ERS)-1 and ERS-2 was the first active sensor that could retrieve SM even though it was primarily designed for monitoring wind. The other active microwave sensors for retrieving surface SM are the Advanced Scatterometers (ASCAT, C-band 5.255 GHz) [169], which are successors of SCAT. There are three operational ASCAT instruments at present: onboard Meteorological Operational satellite-A (MetOp-A) (launched in October 2006), MetOp-B (launched in September 2012), and MetOp-C (launched in November 2018), achieving an approximate revisit time on Earth of 1.5 days. The Sentinel-1 mission is another active microwave observation system for retrieving surface SM at a high spatial resolution (1 km) [69, 122], which is a part of the Global Monitoring for Environment and Security (GMES) program of the European Space Agency (ESA) and the European Commission (EC) [8]. The Sentinel-1 consists of two polar-orbiting C-band synthetic aperture radar (SAR) satellites (Sentinel-1A and Sentinel-1B) launched in April 2014 and April 2016, respectively, and the global revisit time of the 2-satellite constellation is 12 days [122, 165] (Table 1).

Another prominent satellite mission mainly for the measurements of the global SM is the Soil Moisture Active and Passive (SMAP) [55], which was launched on January 7, 2015, by the National Aeronautics and Space Administration (NASA). Since April 2015, various SMAP SM products have been provided at spatial resolutions of 3, 9, and 36 km derived from an L-band radiometer (passive, 1.41 GHz) and a rotating reflector radar (active, 1.26 GHz). However, only radiometer-derived products have been available till now since the radar stopped transmitting in July 2015 because of a component failure. The global coverage revisit time and the spatial resolution of the SMAP are around 2–3 days and 40 km, respectively.

2.2 Retrieval Algorithms

The passive and active microwave-derived products are different in terms of the retrieval approaches utilized [167] as well as their performances by spatial resolution, sensitivity to surface conditions [137, 172], and the source of electromagnetic energy used. Radiometers (passive) observe microwave emission from the land surface as brightness temperature, but active sensors detect distance and backscatter by transmitting and receiving pulses of microwave energy. Therefore, retrieval of SM from passive observations involves different approaches from those in active sensors and has distinctive characteristics in spatial resolution and sensitivity to surface conditions. In short, wet soils present cooler brightness temperature (passive, radiometer) and brighter backscatter (active, radar). The passive microwave-derived SM generally has a coarser spatial resolution due to large antenna sizes for capturing the typically weak signal from thermal emission, but they are less sensitive to land surface conditions such as vegetation (sparse to moderate) and surface roughness. On the contrary, the active microwave-derived products tend to have finer spatial resolutions but are difficult to be interpreted through surface backscattering due to their high sensitivity

Table 1 Summary of passive and active microwave sensors related to soil moisture retrievals (selectively updated from Karthikeyan et al. [74] and Walker et al. [172])

Sensing type	Instrument	Satellite/ mission	Mission period	Frequency (GHz)	Incidence angle (°)	Footprint size (km)	Temporal resolution (days)	Spatial coverage
Passive	SMMR	Nimbus 7	October 1978–August 1987	6.6/10.7	50.2	148 × 95/91 × 59	2	Global
	SSM/I	DMSP	August 1987–December 2007	19.3	53.1	70 × 45	1	Global
	TMI	TRMM	December 1997–April 2015	10.7	35	59 × 36	1	40° N–40° S
	AMSR-E	Aqua	June 2002–September 2011	6.9/10.7	55	76 × 44/49 × 28	1	Global
	WindSat	Coriolis	February 2003–July 2012	6.8/10.7	53.5	60 × 40/38 × 25	1	Global
	AMSR2	GCOM-W1	July 2012–present	6.9/10.7	55	62 × 35/42 × 24	1	Global
	MIRAS	SMOS	January 2010–present	1.4	0–55	23–350	1–3	Global
	Aquarius	SAC-D	June 2011–June 2015	1.413	25.8–40.3	76–156	2–3	Global
	MWRI	FengYun-3B	August 2010–present	10.7	55.4	51 × 85	1–2	Global
Active	SCAT	ERS-1/2	July 1991–September 2011	5.3	16–50	50 × 50	2–7	Global
	ASCAT	MetOp-A/B/C	January 2007–present	5.225	25–65	25 × 25	1–2	Global
	C-band SAR	Sentinel-1	April 2014–present	5.410	20–47	Various by modes	6–12	Global
Active + passive	L-band radar/radiometer	SMAP*	January 2015–present	1.4	40	47 × 39	1–3	85.044° N–85.044° S

*Note: The SMAP data is currently only available from the L-band radiometer-derived brightness temperatures because of an irrecoverable malfunction in the radar in July 2015

to the surface conditions. To best utilize these complementary attributes, the SMAP mission combines passive and active microwave observations to retrieve SM at a moderate spatial resolution [55]. A summary of the passive and active retrieval algorithms used is presented in the following subsections.

2.2.1 Passive Microwave Sensors

Microwave radiometry at the X- (8–12 GHz, 3.8–2.5 cm), C- (4–8 GHz, 7.5–3.8 cm), and L-bands (1–2 GHz, 30.0–15.0 cm) are usually used for the SM estimation [37, 55, 61, 75]. Measuring microwave signals is useful in estimating SM in the upper few centimeters of the soil because of the large contrast in dielectric constants of liquid water (~ 80), soil–water mixture (4~40), and dry soil (~ 4), resulting in a corresponding contrast in emission and scattering of microwave radiation [151]. The soil dielectric constant (k) is a complex number comprising of the real part (k') and the imaginary part (k''). The imaginary part represents the energy loss in the soil can usually be ignored when the microwave frequency is low, such as L-, C-, and X-bands [39]. The measurement depths are generally top few centimeters of the soil layer, which represent 10–50% of the wavelength [180] and, therefore, necessitate longer wavelength signals for deeper soil layers. Among the available products, it has been proven that the L-band is physically more suitable than other wavelengths because it has minimal radio frequency interferences (RFI) [172] and has better penetrating capacity through vegetation canopy, and retrieves signals from a relatively deeper soil layer [75, 177]. In spite of the generally lower RFI in the L-band, Zhou et al. [189] recently reported that L-band RFI is concentrated on urbanized areas over China and exhibits high positive correlation with population density. Therefore, it is necessary to pay attention for using L-band-derived SM products around urban areas especially.

The retrieval processes can typically include the two steps of using a radiative transfer model and a dielectric mixing model. In terms of the radiative transfer model (Ulaby et al. [167], the brightness temperature (T_B) is proportional to the surface temperature (T_S) and the soil microwave emissivity (ε). Then the surface emissivity is calculated with relation to the surface reflectivity (Re) according to the Kirchhoff's law as

$$\begin{aligned} T_B &= \varepsilon \times T_S \\ \varepsilon &= 1-R \end{aligned} \quad (1)$$

The surface reflectivity (Re) for smooth soil surface can be estimated by Fresnel's reflectivity equations which are functions of the incidence angle (θ) and the partial dielectric constant (k'). As the surface roughness can directly affect the

satellite-observed brightness temperature thereby reducing their sensitivity to the SM, the roughness parameterizations at global scales remain a challenge despite significant efforts [39, 98, 152, 178].

For vegetated regions, a zeroth-order radiative transfer equation called the tau-omega ($\tau-\omega$) model [111] is generally used to account for the attenuation effects by the vegetation cover and the contributions from the vegetation itself as

$$T_B = \varepsilon_r T_S \Gamma + T_V(1-\omega)(1-\Gamma) + T_V(1-\omega)(1-\Gamma)(1-\varepsilon_r)\Gamma$$
$$\Gamma = e^{-\tau \sec\theta} \quad (2)$$

where Γ is the transmissivity of the vegetation canopy and dependent on the vegetation optical depth (τ) and the incidence angle (θ), and T_S and T_V represent physical temperatures of soil surface and vegetation canopy, respectively; ω is the single scattering albedo; ε_r is the rough surface emissivity. Here, the τ and ω values representing the two vegetation parameters are mainly determined based on vegetation types and amounts.

The dielectric mixing models can then be used to retrieve the SM using the real part of the soil dielectric constant (k'). As the dielectric constant of the soil can also be influenced by the other soil factors, such as the soil texture or the bulk density, the dielectric mixing models commonly involve soil properties affecting the accuracy of SM retrievals. There are two approaches retrieving SM from the soil dielectric constant called by-inverse and by-forward modeling, respectively [73]. The former converts the observed brightness temperatures to SM through the radiative transfer model-dielectric mixing model sequence, and the latter uses the SM data as input to estimate the brightness temperature values in the inverse direction by minimizing the error between estimated and observed brightness temperature values.

2.2.2 Active Microwave Sensors

The active microwave sensors detect the difference between the energy emitted from the instruments and the energy reflected from the Earth's surface, defined as the backscatter coefficient [112]. Surface roughness conditions significantly affect the backscatter coefficient, and the surface roughness is usually characterized by the root mean square height and the correlation [62, 166]. Besides, the sensor configuration also plays a crucial role in retrieving SM from the observed backscatter coefficient. Regarding vegetation attenuation, similar to the passive retrieval algorithms, the vegetation contributions should be excluded from the measured backscatter coefficient. Furthermore, the backscatter coefficient of soil is transferred into the real part of the dielectric constant through the active radiative transfer models, and then the SM retrievals can be estimated using the dielectric mixing model.

Under bare soil conditions, the active radiative transfer model can usually be categorized into three types: physical, semi-empirical, and empirical models [73]. An important physical model is the integral equation model (IEM), which involves some parameters and inputs. It requires as inputs surface roughness parameters that are difficult to measure and collect due to its complex implementation. To overcome the difficulties related to such physical models, semi-empirical models based on the combination of the physical rationale above as well as experimental studies have been developed. Examples of these include the Oh et al. [120] and the Dubois et al. [51] models. Compared to the physical models, the applicable range of the semi-empirical models has been broadened from the pixel scale to a relatively large scale.

According to the relevant validation studies, the algorithms based on these two types of models have their advantages and disadvantages for the retrieval accuracy of the SM products [23, 123]. Unlike the physical and semi-empirical models, some studies are focused on establishing the purely mathematical relationship between the backscatter coefficient and the SM. However, the empirical models are generally inappropriate to retrieve the SM at global scales due to their data requirements and the absence of the physical basis needed.

For vegetated regions, similar to the $\tau-\omega$ model used in the passive retrieval algorithms, the exclusive soil contributions can be retained after filtering out the vegetation contributions on the signals detected by the space-borne microwave sensors. A semi-empirical model called the water cloud model (WCM) [9] has been widely used to eliminate the vegetation effects from the observed backscatter coefficient. At an incidence angle, the WCM separates the co-polarized backscatter coefficient into three terms: the vegetation contribution, the soil contribution, and the interaction of radar radiation between the vegetation and the soil layers, where the last term can be ignored for co-polarized observations [38, 141].

The literature on retrieval algorithms is extensive and evolving. Additional methods using change detection algorithms [113, 114, 170] have been used to calculate the relative SM. The performance of the SM retrievals using the change detection algorithms has been evaluated over the Contiguous United States region and was overall reasonable [74].

3 Evaluation of SM Products

Despite the unique capability of microwave observations for retrieving SM at global scales in near real-time, multiple factors are degrading the performance (Section 2.2). First, the penetration capacity of the microwave is more hindered through denser vegetation and heavier precipitation, resulting in poorer performances. Besides, RFI can contaminate the microwave signals [92, 116, 139]. In addition to this, satellite microwave SM products arise from different instruments and

algorithms [55, 61, 70, 75, 118, 121], resulting in differences in their performances. In other words, uncertainties exist in the products due to many complex factors affecting the SM retrievals, including imperfect retrieval algorithms, measurement errors, and uncertainties in the limited parameterizations of land surface roughness and vegetation [129]. The retrieval algorithms link the remotely sensed microwave observations to SM values and generally introduce uncertainty due to methods and model parameterization used in the retrieval algorithms. The measurement error is defined as the difference between a measured SM value and its true value and consists of random and systematic errors. The random error is caused by any random factors such as accuracy limits of the measuring instrument. The systematic error results from any systematic factors like incorrect calibration of the measurement instrument [64] and an uncorrected dynamic open water fraction within the sensor footprint which generally causes a strong positive bias. In addition to this, there are also systematic differences between ground-based and satellite-derived SM. These differences result from various sources including the spatial representation of the ground-based observations (i.e., point-scale), differences in measurement depth of the in situ sensor, and the microwave emission [29].

The need for accurate SM products is evident for various applications including weather prediction [49] and flood forecasting [15]. Therefore, it is essential when using or improving SM products to identify their error characteristics in time and space through a suitably designed evaluation or validation procedure.

Generally, there are two approaches are available at present. These are using ground-based observations as reference (referred to as "traditional approach") and applying advanced techniques to overcome limits of the traditional approach (referred to as "advanced approach"). Subsections 3.1 and 3.2 describe the details of the two approaches and their advantages and disadvantages.

3.1 Traditional Approach

A SM product (θ_{est}) is traditionally evaluated in comparison with ground-based observations regarded as the assumed truth (θ_{true}) and, generally, uses metrics such as bias, root mean square error (RMSE), unbiased RMSE (ubRMSE), and correlation coefficient (R) [48, 56, 185], as per Eqs. (3)–(6).

$$\text{bias} = E[\theta_{est}] - E[\theta_{true}] \tag{3}$$

$$\text{RMSE} = \sqrt{E\left[(\theta_{est} - \theta_{ture})^2\right]} \tag{4}$$

$$\text{ubRMSE} = \sqrt{\text{RMSE}^2 - \text{bias}^2} \tag{5}$$

$$R = \frac{E[(\theta_{est} - E[\theta_{est}])(\theta_{true} - E[\theta_{true}])]}{\sigma_{est}\sigma_{true}} \tag{6}$$

where $E[\ldots]$ represents the arithmetic mean of the data, and σ_{est} and σ_{true} are the standard deviations of the SM product and the assumed truth, respectively.

Preprocessing of remotely sensed SM is commonly applied for many applications. This is a prerequisite to minimize the systematic differences that would otherwise occur [145]. Preprocessing steps include restricting the maximum measurement depth of the ground measurements being used, applying a quality control procedure [46], and/or checking the area representativeness of stations by considering independent data [43, 184]. Such preprocessing is often achieved by removing the climatology and/or scaling to match the unique model SM climatology [145].

The International Soil Moisture Network (ISMN) is an important contribution to validation works using ground-based SM (http://ismn.geo.tuwien.ac.at/) [45]. The ISMN is a centralized data hosting system which collects global SM measurements from various networks, processes, and releases the data to users. As of April 2019, the ISMN consists of 2439 ground stations from 59 networks mainly distributed over the USA and Europe as presented in Fig. 2. The ISMN ground measurements have been widely used for validation studies [79, 132, 183]. Recently, Zhang et al. [188] evaluated the SMAP Enhanced Level-3 Soil Moisture product using ground measurements from 191 ISMN stations distributed over various conditions and presented how the SMAP product performs over the conditions. Al-Yaari et al. [1] evaluated various SM products using the ISMN datasets over different ecoregions, land cover types, and climate conditions.

3.2 Advanced Approach

As the traditional approach using ground-based measurements is spatially limited and presents systematic differences against satellite-derived products, the need for alternate validation techniques has been felt. One way to overcome this limitation has been the direct comparison with other independent SM products derived from different satellite instruments and/or retrieval algorithms or land surface (reanalysis) products, which have similar spatial resolutions with the satellite-derived products to be compared. For example, Hain et al. [68] compared yearly temporal correlation coefficients between seasonal anomalies of two datasets among three SM products derived from passive microwave, thermal infrared, and a land surface model over the continental USA, the correlations being moderate to strong against each other during a near-decadal period adopted. Another example of using an independent data product is presented in Dorigo et al. [42]. In the study, temporal correlation coefficients at a global scale between a four-decade SM product, called European Space Agency Climate Change Initiative Soil Moisture (EAS CCI SM), and a reanalysis surface SM product were calculated.

Fig. 2 Distribution of ground stations for measuring soil moisture from ISMN consisting of 2439 ground stations from 59 networks (April 2019)

Crow [28] introduced the R_{value} method for large-scale verification applications, which has since been frequently used for evaluating remotely sensed SM products without using ground-based SM observations [30, 33, 126, 127]. The R_{value} method is initiated from a simple linear state model to predict the antecedent precipitation index (API) using satellite-derived precipitation (P) for the past select timesteps using γ as a calibrated API loss coefficient.

$$\text{API}_k = \gamma \text{API}_{k-1} + P_k \tag{7}$$

Thereafter, a Kalman filter optimally updates an API ("+") by assimilating satellite SM data (θ_s) into a model-predicted API ("−") through Eq. (7) at time k.

$$\text{API}_k^+ = \text{API}_k^- + K_k\left(\theta_s - \hat{\theta}\right) \tag{8}$$

where $\hat{\theta}$ is the predicted SM as a function of API_k^- (i.e.,) , and Kalman filter analysis increments (I) are defined as the second term of the right-hand side (i.e., $I = K_k\left(\theta_s - \hat{\theta}\right)$). Here, Kalman gain (K) is a function of the errors from the API model (Eq. (7)) and satellite SM and determines the degree of adjustment of API by the residual term, $\left(\theta_s - \hat{\theta}\right)$. The temporal behavior of the Kalman filter analysis increments (I) tends to be inverse against the satellite precipitation error (E, assumed as known information using ground measurements) for complementing the satellite precipitation error-derived degradation in the API estimation by the Kalman filter process. In other words, the more positive the error E is, the more negative I is, and vice versa. The idea of the R_{value} method is that the inverse tendency between E and I can be contrasted if the satellite SM has a better performance. R_{value} is defined to be the negative temporal correlation coefficient between E and I (R) and typically ranges from 0 to 0.7.

$$R_{\text{value}} = -R \tag{9}$$

Despite the applicability, the R_{value} method has some limitations: (1) it relies on the simple linear model (i.e., API) for predicting SM in the Kalman filter process; (2) it can only evaluate temporal correspondence of the SM products; and (3) it needs spatially representative and high-quality ground-based rainfall measurements to properly define the satellite precipitation error [28, 30, 33].

Another large-scale verification technique is the triple collocation (TC) [156]. TC is a statistical tool for estimating the variance of the random error term from triplet datasets (e.g., SM) without a high-quality reference dataset. The TC method was extended to estimate the data–truth correlations (R) as well as the signal-to-noise ratio (SNR) [66, 108].

Since Stoffelen [156] used TC for evaluating error characteristics for wind vector data, TC has been frequently used for evaluating SM datasets from various sources such as passive/active microwave and models. For example, Scipal et al. [153] applied the TC for passive and active microwave-derived and reanalysis SM products, and Dorigo et al. [43] also applied the TC technique to assess random errors in CCI SM. Kim et al. [78] evaluated passive (AMSR2), active (ASCAT), and passive-active (SMAP) microwave-derived SM products at a global scale using TC and presented their performances by vegetation density. Chen et al. [20] assessed SMAP, SMOS, and ASCAT SM products at a global scale using TC in terms of anomaly temporal correlation.

Despite the usefulness of TC, it has also faced challenges in overcoming inherent assumptions and data availability limitations. There are unique assumptions in TC analysis including (1) linearity between the truth and the observed data (i.e., truth + error); (2) stationarity for both the truth and the error; (3) orthogonality, meaning the errors are independent from the truth; and (4) error cross-covariance independence. Many efforts have been devoted to investigating these assumptions. For example, nonlinearity between the observation and the truth was identified by Su and Ryu [160], but Crow and Wood [32] found that there are linear correlations between coarse-scale SM observations. Dynamic TC has been also examined to overcome the stationarity assumption [101], but such nonstationarity studies have been limited by short data availability and missing data [66, 190]. Yilmaz and Crow [186] evaluated the cross-covariances between SM errors and ground data. They suggested that the error cross-covariance is more important than the orthogonality assumption. More details of these assumptions can be found in Gruber et al. [66]. The TC analysis requires three independent data which are often not available in practice. To tackle this problem, Su et al. [158] proposed the single instrumental variable (IVs) method using only two independent products to estimate error variances and data–truth correlations. The IVs uses a 1-day lag time series of one product as the third variable. Further to this, Dong et al. [40] developed the double instrumental variables method (IVd) which uses two 1-day lag time series derived from the two products to get more stable results.

4 Improvement in SM Products

4.1 Accuracy

Satellite-derived SM products need a minimal level of accuracy to be used for various hydrological applications [173]. Aside from advances in the retrieval algorithms and instruments, efforts to improve the accuracy of satellite-derived SM products can be categorized into two techniques: merging of existing SM products and mathematical denoising approaches.

The rationale of merging products is that every product has relative strengths and weaknesses compared to others, and therefore, a product can be supported by other products and made more reliable through judicious combination algorithms. In this direction, Kim et al. [80] investigated key differences in SM retrieval algorithms as a means to understand why different retrievals from the same satellite sensor can lead to major differences in the derived values. These differences were then used to develop new alternatives for combining alternate SM fields representing the same domain, as a means of deriving a better product that is stable and consistent. The complementarity among various SM products has led to better performances in the merged products than the parent (original) ones as presented in the following examples. Liu et al. [99] developed an algorithm for merging multiple SM products derived from various passive and active microwave sensors through which systematic differences among the products are removed through cumulative distribution function (CDF) matching. Kim et al. [82] presented a linear combination-based approach for improving satellite SM products with combination weights derived so as to maximize Pearson correlation (R) to a reference dataset, and Kim et al. [78] applied the maximizing R method for combining pairs of passive, active, and passive–active microwave-derived SM products by which the possibility was presented to overcome limitations of individual SM products over difficult-retrieval regions. Tomer et al. [164] proposed an algorithm to merge the strengths of active (high spatial resolution) and passive (high temporal resolution) SM products. The algorithm sequentially converts a temporal differential of the passive SM to a SM value at the finer spatial (active) and temporal (passive) resolutions by using spatiotemporal changes of the active SM and spatial heterogeneity. Enenkel et al. [53] presented a method to combine active and passive SM products in near real-time based on a global vegetation density by which active sensors, passive sensors, and the average of both are used to generate the near real-time product. Gruber et al. [65] proposed a linear merging scheme which weights the original products based on TC-derived error variances among satellite and model-derived products.

Another way to improve the accuracy of satellite-derived SM products is mathematical denoising of the retrievals. For example, Du [50] applied Fourier analysis to a time series of SM for detecting high-frequency components that reflect SM changes (i.e., anomalies). Based on the extracted high-frequency components, long-term datasets were generated showing a better accuracy through validation using field sampled SM. Another example is presented in Su et al. [159]. In the study, a semi-empirical model was presented based on a power spectral density analysis of SM time series. Based on the semi-empirical model, causal and noncausal filters were systematically designed to remove erroneous signals in the time series, by which substantive increases in linear correlations were shown through evaluations using ground data. In sequence, Su et al. [157] applied the denoising filters to improve passive and active SM products, and Su and Ryu [160] also presented that nonlinear bias correction and denoising can be simultaneously implemented for scale-dependent biases of in situ, satellite, and modeled SM. Lastly, Kornelsen and Coulibaly [86] tried to reduce the multiplicative bias of satellite SM by a few methods such as CDF matching, linear rescaling, and copulas.

4.2 Spatial Resolution

Most satellite-derived SM products have coarse spatial resolutions (> 100 km^2) because larger antenna (aperture) sizes are required for finer resolution, and it has been a technical challenge to launch and operate such large antennas in space. Although the active remote sensing system, especially the SAR, can provide high spatial resolutions (< 1 km), it results in longer revisit times (> 10 days). One generally requires SM data at temporal and spatial resolutions less than a week and 10 km, respectively, for regional hydrological and agricultural applications [150]. Given these limits, various attempts to spatially disaggregate the coarse SM data to finer spatial resolutions have been reported. Recently, Sabaghy et al. [150] categorized such disaggregation methods into active/passive microwave and optical-based, soil surface attribute-based, and model/data-based techniques and comprehensively reviewed their theoretical backgrounds, strengths/weaknesses, and reported performances. Those techniques include statistical methods such as kriging or fractal interpolation [77, 100], along with the use of complementary information such as topographic/soil properties [134], land surface temperature, vegetation, and soil evaporative efficiency derived from high spatial resolution optical/thermal infrared sensors, land surface model, and radar [58, 110, 115, 136, 140].

These methods, using complementarity in the sensors, have developed relationships among microwave-derived SM at a coarse spatial resolution and climatological data such as land surface temperature (LST) and vegetation index (VI) available at both coarse and finer spatial resolutions. Simply stated, these methods generally establish a relationship between the SM and climatological data at the coarse spatial resolution through physical/statistical approaches, and then the established relationship (function) is used to calculate SM data at the finer resolution based on the climatological input at the finer resolution. Following this, biases of the calculated SM data at the finer resolution are linearly scaled so that their spatial average is identical to the coarse SM over the corresponding fine grid cells. For example, Fang et al. [59] suggested a method which uses look-up tables to relate the datasets at the coarse spatial scale to the daily temperature difference at a finer spatial scale to give the daily average SM at the finer scale. Peng et al. [136] proposed a SM disaggregation method by using the vegetation temperature condition index (VTCI) as a SM proxy. When plotting paired LST and VI over an area for a period, the data generally forms a triangular or trapezoidal shape which is called the LST/VI feature space where a degree change in surface wetness is stipulated by a pairwise change in LST and VI at a location within the area, called VTCI [174]. For the latter set of approaches that rely on complementary surface information, one of the key issues to overcome has been the cloud masks on optical/thermal infrared sensor-derived data. Such masks tend to cause large gaps in the disaggregated SM and therefore decrease the usability of the SM dataset. To overcome this limitation, Kim et al. [79] presented a disaggregation approach to spatially disaggregate coarse SM by only using remotely sensed vegetation index, which is based on the conditional relationship of vegetation with time-aggregated SM. This approach, additionally, imparted persistence between soil moisture across adjacent time steps, a limitation that has been existing in past SM disaggregation approaches till date. Further details about the spatial disaggregation of satellite-derived SM are well presented in recently published review papers [135, 150].

5 Applications for Flood Estimation and Monitoring

Satellite remote sensing is useful to forecast and monitor the evolution of flood events in space and time. For example, the 2010 catastrophic flood in Pakistan resulted in more than 2000 deaths and severe economic damage [162]. As shown in Fig. 3 a–d, the temporal evolution of the flooding can be well characterized by the spatiotemporal distributions of satellite-derived SM. Even at the coarse spatial resolution of 0.25° (approximately 25 km at the equator), one can observe changes in SM images from preflood conditions (July 10), to peak flood conditions (July 28–August 4) and inundation conditions (August 13). As the event progressed, SM levels steadily increased, leading to more precipitation and finally causing the extensive inundation (Fig. 3e–i). At the same time, high SM also increased the resulting flood magnitude as antecedent moisture preceding rainfall resulted in more water becoming surface runoff.

Given that satellite-derived SM products can be a good indicator of surface wetness, their use has been widely investigated for flood estimation or monitoring in past decades. In this paper, such investigations are categorized into four sets of approaches as summarized in Table 2, namely (1) model parameter calibration, (2) data assimilation (DA) and (3) combination of rainfall correction and DA for flood estimation, and (4) flood monitoring using satellite-derived SM or satellite-observed microwave brightness temperature.

5.1 Applications

First, remotely sensed SM is included in model calibration to estimate more reliable model parameters, which in turn improves flood forecasting [102, 175]. Traditional model calibration estimates parameters by minimizing discrepancies between simulated discharge and observed streamflow. Including spatial distribution of satellite-derived SM can introduce more valuable information to constrain model parameter estimations compared to calibration on only discharge [85, 125]. However, such studies also found that reductions

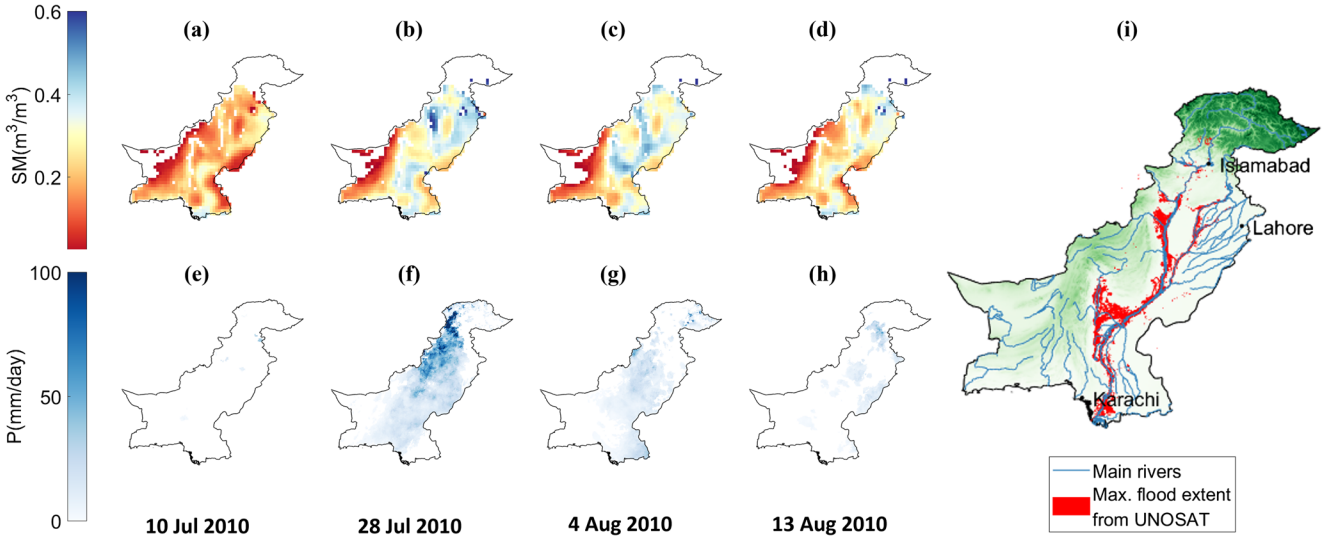

Fig. 3 Spatiotemporal distributions of (**a**–**d**) soil moisture derived from AMSR-E at 0.25°, **e**–**h** rainfall from CHIRPS final product at 0.05° (http://chg.geog.ucsb.edu/data/chirps/), and **i** maximum flood extent records from UNOSAT (http://www.unitar.org/unosat/)

of uncertainty in SM states without degradation of predicted streamflow were found in certain cases of model calibration using satellite-derived SM. The explanation of this finding could be the model structure complexity in which lumped or semidistributed models are simple and cannot represent spatial variations of satellite-derived SM, and hence, do not improve predicted discharge [6, 22]. Therefore, distributed models have been given increased attention to improving predicted streamflow by calibration using remote sensing SM. For example, Wanders et al. [175] and Silvestro et al. [154] found that joint calibration on both discharge and SM can improve simulations of streamflow and provide accurate and reliable model parameters. These studies also highlighted that more robust model parameter estimation using satellite SM was found in sparsely gauged regions. To overcome the impact of limited data availability and computational costs for hydrological modeling, Kim et al. [81] presented a method for identifying flood risk at a location within a watershed using satellite-derived SM and open-access information for rainfall, soil properties, and a digital elevation model. The outcomes of the model performance showed promise in contingency table-based skill scores, where the Pearson correlation and Peirce skill score (PSS) [181] values were found to be comparable to the results from the Global Flood Awareness System (GloFAS) [4]. Other findings of applications of SM in model calibration are presented in Table 2.

The second type of application for flood estimation is assimilating satellite-derived SM into hydrologic models to update model states to reduce uncertainty in initial conditions and improve flood prediction. SM is a crucial initial condition for rainfall–runoff models. Accuracy of initial condition is very sensitive to errors of model outputs. Assumption of constant initial condition will lead to incorrect forecasts of streamflow. Therefore, assimilation of satellite-derived SM into hydrologic models to update the initial conditions of models has been noted by many studies in the last two decades. Various DA techniques including particle filter (PF), ensemble Kalman filter (EnKF), and nudging have been used to assimilate different temporal scales (hourly to daily) of remote sensing SM into different complexity of model structure (lumped, semi-distributed, and distributed). Li et al. [94] suggested that the EnKF algorithm had better computational efficiency and bias reductions compared to the PF algorithm. However, finding the most suitable DA technique using satellite-derived SM for different model structures is still a question. In a flood forecasting perspective, high frequent remote sensing SM is required for near real-time flood prediction. Consequently, assimilations of the current satellite SM missions (AMSR-E, AMSR-2, ASCAT, SMOS, or SMAP) with subdaily temporal resolution have been widely used [96]. In terms of model structures, physical-based or grid-based models simulate streamflow in fully distributed subcatchments or catchments, whereas conceptual or empirical models tend to aggregate spatial information of satellite SM into catchment systems [147]. Although the distributed models can benefit from spatial information of satellite SM, lumped and semidistributed models are still used for flood forecasting because of computational efficiency. Therefore, it is required to develop efficient and robust approaches for updating SM states in conceptual models [6]. As discussed above, there are many problems in DA techniques using satellite-derived SM to improve flood forecasting, and tremendous efforts have been devoted to improving understanding of assimilation of satellite SM into flood models. Investigations have found that joint assimilation of SM and discharge outperformed single assimilation of either SM or discharge [6, 15, 16, 26, 90, 103, 176], whereas other investigations have indicated that assimilation of SM resulted in negative/small positive impacts on prediction of streamflow [22, 106, 138]. To investigate these inconsistent results, the catchment

Table 2 Summary of satellite soil moisture (SM) applications in hydrologic models to improve flood forecasting. These studies were allocated with respect to four common approaches (model parameter calibration (Cal.), data assimilation (DA), combination of rainfall correction and data assimilation (Com.), and flood monitoring (FM). Other acronyms and abbreviations can be found in the main texts and/or the Appendix)

Approach	Instrument/ mission/SM data	Model/method	Study area	Key finding	Reference
Cal.	SM data measured from the Southern Great Plains 1997 experiment in Oklahoma	Soil Conservation Service (SCS) curve number (CN) method	Five catchments in the Little Washita watershed	• Remotely sensed SM data were used for defining antecedent soil moisture conditions in the SCS CN method • Significantly reduced errors in rainfall–runoff predictions compared to the standard SCS method	Jacobs et al. [71]
Cal.	AMSR-E, ASCAT, SMOS	LISFLOOD	Upper Danube catchment, Europe	• Calibration of both discharge and SM improves discharge simulation compared to calibration only on discharge	Wanders et al. [175]
Cal.	H-SAF	Continuum	Orba and Casentino catchments, Italy	• Calibration on both ground stations (discharge) and satellite data (SM and land surface temperature) reduces the number of equifinal solutions	Silvestro et al. [154]
Cal.	AMSR-E	SWAT	Upper Wabash and Cedar Creek catchments, USA	• Root-zone SM is crucial for model calibration • Model parameters have reduced the range of uncertainty in subsurface processes	Rajib et al. [142]
Cal.	Sentinel-1	HEC-HMS	Keramianos Basin, Greece	• Topsoil SM content was estimated by using images from Sentinel-1 and Landsat 8 • The estimated SM was used for defining the initial soil condition in hydrologic simulations using HEC-HMS • Promising simulation results in flow time series	Alexakis et al. [3]
Cal.	AMSR-E	AWRA-L	11 catchments, Eastern Australia	• Calibration performs well for catchments with medium to high average flows	López et al. [102]
Cal.	SMOS	GRKAL (GR models)	Clarece River and Condamine River, Southeast Australia	• At sites not used for the calibration, the spatial distribution of SM led to significant improvement • Using SM for calibration at upstream and tributary subcatchments had better results compared to downstream subcatchments	Li et al. [93]
Cal.	ESA CCI SM, SMAP	Developed model	65 catchments, Murray–Darling Basin, Australia	• Promise in flood warning skill scores comparable with GloFAS results over Murray–Darling Basin	Kim et al. [81]
DA	TMI	API-SM	USA	• Assimilation of SM into an API SM proxy can improve predictive skill of land surface response to rainfall	Crow et al. [26]
DA	AMSR-E	SAC-SMA	MOPEX basins, USA	• SM retrievals can improve estimates of both rainfall accumulations and antecedent SM conditions • Dual SM-DA of storm-scale rainfall and prestorm SM outperforms SM-DA of antecedent SM conditions in flow predictions	Crow and Ryu [31]
DA	ASCAT	MISDc	Upper Tiber River, Central Italy	• Assimilation SM in soil wetness index can provide valuable initial soil wetness conditions to improve runoff prediction	Brocca et al. [15]
DA	ASCAT	SIM	France	• Directly removing precipitation bias would be more effective than correcting it by SM-DA	Draper et al. [47]
DA	Synthetic data	SWAT	Cobb Creek catchment, Oklahoma, USA	• Model problems prevent SM-DA from improving discharge predictions	Chen et al. [22]
DA	ASCAT	MISDc-2L	Central Italy	• Significant improvement of discharge prediction can be achieved by assimilation both the surface and root-zone SM	Brocca et al. [16]

Table 2 (continued)

Approach	Instrument/ mission/SM data	Model/method	Study area	Key finding	Reference
DA	ASCAT	BibModel	Bibesch catchments, Grand Duchy, Luxembourg	• Assimilation of few in situ SM sites over a catchment can improved both discharge and soil wetness forecasts • Assimilation of satellite-based SM led to a negative or small positive impact • SM-DA is the most efficient in transitional season periods (wet–dry conditions)	Matgen et al. [106]
DA	AMSR-E	PDM	Warrego River, Australia	• Assimilation of SM has less skill when there are high biases in the peak flow prediction • Rescaling SM is important for the data assimilation efficacy	Alvarez-Garreton et al. [5]
DA	ASCAT, AMSR-E, ERA-Land Reanalysis	SCRRM	Rafina River, eastern Attica region, Greece	• Using SM as indicator for the flood model provides better results than the model using initial condition	Massari et al. [103]
DA	SMOS	MIKE SHE SWET	Ahlergaarde River, Western Denmark	• Assimilation of satellite SM data improves SM correlations compared to in situ SM for most land covers • Improvement is found at topsoil layer but degradation is found at shallow soil layer	Ridler et al. [147]
DA	ASCAT, AMSR-E, SMOS	LISFLOOD	Upper Danube catchment, Europe	• SM-DA improved performance of baseflow prediction and reduced uncertainty in the overall discharge • Joint assimilation of SM and river discharge outperformed single assimilation of river discharge • SM-DA reduces timing errors in the flood predictions	Wanders et al. [176]
DA	AMSR-E, ASCAT, SMOS	PDM	4 arid catchments, Australia	• SM-DA efficacy is improved when accounting for the spatial distribution in forcing data and routing processes • SM is effective for improving streamflow ensemble prediction at ungauged sites	Alvarez-Garreton et al. [6]
DA	SMOS	VIC	Murray–Darling River, Australia	• First-order bias correction (rescaling of the long-term mean) preserving the variability of SM data that leads to improve state for dry and wet conditions • Second or high order (rescaling of variance) decreases the temporal variability of the data assimilation results	Lievens et al. [97]
DA	ASCAT	MISDc	Tiber River catchment, Central Italy	• SM-DA should be carefully tested with different catchment characteristics (e.g., area, soil type, climatology, rescaling method, observation and model error selection)	Massari et al. [105]
DA	ASCAT, H-SAF	Continuum	Orba, Casentino, and Magra catchments, Italy	• The impact of the SM-DA strongly replies on the permanent catchment characteristics (topography, hydrography, or land cover)	Cenci et al. [19]
DA	SMOS, H-SAF	Continuum	Orba catchment, Italy	• SM-DA has substantially impact on wet seasons • Both finer resolution geostationary SM in a small basin and coarse resolution satellite SM can improve discharge prediction	Laiolo et al. [90]
DA	Synthetic data	XAJ	–	• SM-DA accounting for the runoff routing lag has significant improvement compared to SM-DA without considering runoff routing lag	Meng et al. [109]
DA	ESA CCI SM	AWRA-L	6 catchments, Australia	• SM-DA slightly improves evapotranspiration prediction but degrades discharge prediction	Pham et al. [138]

Table 2 (continued)

Approach	Instrument/ mission/SM data	Model/method	Study area	Key finding	Reference
				• Joint assimilation of multiple observations can improve model performances compared to open-loop simulation	
DA	SMOS, AMSR-E	SAC-SMA	Warwick, Australia	• Jointly estimated rainfall and model parameters improved streamflow prediction	Wright et al. [182]
Com.	ASCAT, SMOS	SAC-SMA	13 catchments, USA	• Rainfall forcing input correction is more efficient in improving high flow prediction • Corrected prestorm SM state is able to improve baseflow • Both high and low flow predictions are improved through dual assimilation of corrected forcing and state • SM-DA results in underprediction of extreme flow events	Chen et al. [21]
Com.	AMSR-E/LSMEM	VIC	USA	• SM retrievals provide useful information to correct precipitation biases • Medium rainfall is corrected effectively for dry to normal surface • Rainfall correction has negative improvement over wet surface • High variance SM introduces more noise in rainfall forcing especially over wet regions	Zhan et al. [187]
Com.	ASCAT, AMSR-E, SMOS	PDM	4 arid catchments, Australia	• Corrected medium and high daily rainfall forcing leads to improvement of discharge predictions • Single SM-DA outperforms for rainfall correction	Alvarez-Garreton et al. [7]
FM	SSM/I	SI, PI, FI	China	• Proposed regional threshold value (F0) for monitoring regional floods (When FI < F0) • F0 can be determined empirically from the local flooding statistics and comparison with satellite data	Jin [72]
FM	AMSU	SWVI	Carpathian Basin, Hungary	• SWVI tested on a flooding event in Hungary, which was efficient for monitoring soil wetness variations	Lacava et al. [89]
FM	AMSR-E	NASA Level 3 SM product	Gujarat and Rajasthan, India	• Presented regional threshold values for SM to estimate flood-affected area in India • Rainfall pattern and flooded area correlates well during the rainy season	Rao and Sharma [143]
FM	AMSR-E	*MC* ratio	6 river reaches, USA	• *MC* ratio is sensitive to dynamics of soil moisture and water fraction on the land surface	Brakenridge et al. [13]
FM	SSM/I, SCAT, AVHRR	Global monthly mean inundation extent maps	Ob, Yenissey, and Lena catchments, Russia	• Monthly satellite-derived inundation has a good agreement with streamflow processes in the Arctic regions	Papa et al. [124]
FM	AMSR-E, MODIS, SRTM DEM	BWI	Peace Athabasca Delta, Canada	• BWI uses regional topographic information to separate effects of soil wetness and open waterbodies from observed passive microwave signals • BWI presented a better capability to capture the soil wetness over a catchment in Canada	Temimi et al. [163]

characteristics, the routing lag, or the SM data preprocessing has been considered as possible factors requiring improved specifications [5, 19, 97, 105, 109].

Thirdly, satellite SM can be integrated into hydrologic models through simultaneous assimilation of SM and rainfall correction. Due to strong connections between SM and rainfall, SM data were used to correct rainfall [14, 27, 87, 133, 148]. The corrected rainfall model and the updated SM states were assimilated simultaneously to improve flood predictions. Key findings of the dual assimilation of SM and rainfall correction approach are summarized in Table 2. The combination approach of using corrected forcing input and updated SM states can reduce uncertainty in initial conditions and, hence, improve streamflow prediction [21].

Lastly, other applications involve using satellite-observed microwave brightness temperature for flood monitoring based on physical relationships rather than directly using SM products. During the last two decades, there have been a series of efforts to develop passive microwave-derived soil wetness indices with relation to flood monitoring. For example, Jin [72] proposed a simple flooding index using differences in passive microwave observations from different frequencies and polarizations and suggested regional thresholds of the index for flood monitoring below which flooding is considered to occur. Lacava et al. [89] presented a passive microwave-based flood index for improved monitoring of soil wetness variations concerning a flood in Hungary in 2000. Rao and Sharma [143] used thresholds of a passive microwave-derived SM product for estimating the affected flood extents in watersheds in India. Temimi et al. [163] presented an index called basin wetness index (BWI) for an improved soil wetness monitoring over a catchment in Canada. It was shown that BWI presented a better capability to capture the soil wetness over a catchment in Canada, which was done by minimizing the effects of open waterbodies on passive microwave signals with regional topographic information derived from a digital elevation model.

As an alternative to ground-based flowrate data, Brakenridge et al. [13] developed a passive microwave-derived flood signal, called measurement–calibration (*MC*) ratio, the ratio of brightness temperature over wet measurement (*M*) and dry calibration (*C*) pixels. It has been known that the *MC* ratio is highly correlated with high flowrates and so widely used and tested for various hydrologic applications, including flood monitoring and model parameter estimation [35, 76].

5.2 Limitations

Although satellite-derived SM has provided additional information for more reliable and robust flood estimation and monitoring, there are still challenges. First of all, the use of spatial information of satellite SM suffers from differences in spatial scales and soil layers between satellite observations and model configuration. Satellite SM provides grid-based with topsoil layers, whereas conceptual models are lumped catchment systems with single soil layers. Although there are different approaches to propagate satellite SM into conceptual models such as using external models to introduce a topsoil layer [16, 60] or using exponential filtering algorithms [6, 154], there are still discrepancies between aggregated satellite SM and simulated SM. This bias could lead to overcorrection of SM states and degradation of streamflow prediction. There have been many efforts done in bias correction of satellite SM such as using cumulative distribution function [15, 161] or sequential processes of calibration and assimilation [175]. However, there are still potential avenues for investigation of parallel tasks of bias correction and assimilation of remote sensing SM to hydrological models [97, 147].

SM observation errors play important roles in data assimilation techniques, but uncertainty quantification of satellite SM is frequently difficult. This is because there are different soil layer observations (systematic errors) between satellite and in situ SM data or simulated SM. Moreover, systematic errors among multiple satellite SM missions result in challenges in merging of multisource of remote sensing SM for flood applications. Furthermore, propagation of model uncertainties into model output in DA procedures has not been received with sufficient attention [6]. Future work should focus on simultaneously integrating model uncertainty and observational errors to improve flood forecasting. One possible approach is to use the triple collocation (Section 3.2) for the simultaneous estimation of model and observational errors.

Despite the potential of using satellite-derived SM or satellite-observed microwave brightness temperature for flood

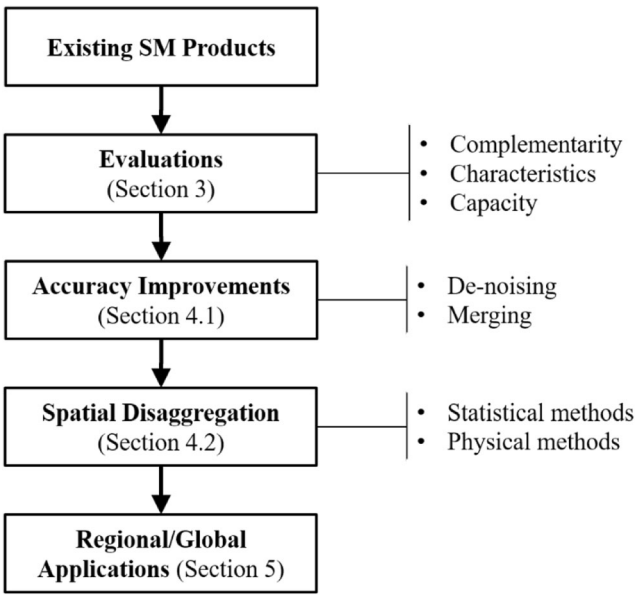

Fig. 4 Schematic diagram presenting an integrated pathway for developing improved soil moisture data

monitoring, there are still open questions regarding the inherent uncertainties and coarse spatial resolutions that have been consistently discussed in this paper. For example, the geographically fixed measurement grid cells of the satellite measurements do not always guarantee favorable conditions for flood monitoring over an area of interest [12], and the accuracy of the approaches is hard to meet for small catchments because of the coarse grid sizes with tens of kilometers [76]. Therefore, it should be noted that such efforts to address the above questions are to be in parallel with the applications. As examples for this, Revilla-Romero et al. [146] evaluated the *MC* ratio by using flowrate data from hundreds of stations over the world and provided guidelines on how it should be used based on identified dominant factors influencing the performance. Kim and Sharma [83] presented an approach for improving the *MC* ratio by accounting for local topography within a catchment by which clear improvements were achieved compared to using the raw data.

Lastly, there still exist a number of issues that make their use in real-time challenging for flood estimation and monitoring. While the quality of satellite retrievals is improving, more needs to be done especially on the ground measurements so that better retrieval alternatives can be derived, and physical relationships remedied. Having said so, the accuracy of flood warning schemes using satellite retrievals alone is improving, as is demonstrated by the results of Kim et al. [81]. With improvements in other remotely sensed measurements (including precipitation extremes as in Libertino et al. [95]), the future for effective flood warnings in remote underdeveloped countries is bright.

6 Conclusions and Outlook

Assessing flood risk over sparsely gauged or ungauged basins generally requires a methodology for forecasting, along with key information resources (rainfall and SM) that could be made available without delay (and expenditure) for use in remote locations around the world. The spatiotemporal availability of (active and/or passive) microwave-derived SM products in near real-time at global scales was identified as a viable alternative to ground measurements, with improvements still being required for which various efforts are underway.

In this context, this paper briefly introduced the four-decade chronology of satellite-derived SM data together with main characteristics of the two types of SM retrieval algorithm using passive and active microwave observations and introduced the traditional and advanced techniques for validating the SM products and discussed their advantages and disadvantages. Then we reviewed the literature devoted to redressing drawbacks in terms of accuracy and spatial resolution as well as uses of satellite SM products for assessing flood risk. Together with this, this paper argues that it is important to have adequate spatiotemporal information on SM to improve hydrological forecasting capacities. Ongoing and future research will form an integrated pathway (Fig. 4) for producing an improved SM product available at finer spatial resolutions, which can be used for various regional applications. Based on this, it is also worthwhile to develop long-term and consistent global soil moisture data (e.g., EAS CCI SM, Section 3.2), which can provide improved flood forecasting capacity.

Acknowledgments This paper was structured based on the thesis of Seokhyeon Kim titled "Improvements and Applications of Satellite-Derived Soil Moisture Data for Flood Forecasting" in fulfillment of the requirements for the degree of Doctor of Philosophy (Ph.D.) from the University of New South Wales (UNSW), Sydney, Australia in 2017.

Funding Information Seokhyeon Kim's Ph.D. project has been conducted as a part of a Discovery project (DP140102394) funded by the Australian Research Council. The authors would like to acknowledge UNSW contributions to a postgraduate scholarship for Seokhyeon Kim to pursue his Ph.D.

Appendix Acronyms and Abbreviations

AMSR2	Advanced Microwave Scanning Radiometer 2
AMSR-E	Advanced Microwave Scanning Radiometer for the Earth Observing System
AMSU	Advanced microwave sounding unit
API	Antecedent precipitation index
ASCAT	Advanced scatterometers
AVHRR	Advanced very high resolution radiometer
AWRA-L	Australian Water Resource Assessment Landscape
BWI	Basin wetness index
CDF	Cumulative distribution function
CHIRPS	Climate Hazards Group InfraRed Precipitation with Station
CRED	Centre for Research on the Epidemiology of Disasters

DA	Data assimilation
DSMP	Defense Meteorological Satellite Program
EC	European Commission
EnKF	Ensemble Kalman filter
ERA-Land	European Centre for Medium-Range Weather Forecasts (ECMWF) ReAnalysis-Land
ERS-1/2	European Remote Sensing-1/2
ESA	European Space Agency
ESA CCI	European Space Agency Climate Change Initiative
FI	Flooding index
GCMO-W1	Global Change Observation Mission-Water 1
GEMS	Global Monitoring for Environment and Security
GloFAS	Global Flood Awareness System
GR model	French: modèle du Génie Rural
HEC-HMS	Hydrologic Engineering Center - Hydrologic Modeling System
H-SAF	Satellite Application Facility on Support to Operational Hydrology and Water Management
IEM	Integral equation model
ISMN	International Soil Moisture Network
LSMEM	Land surface microwave emission model
LST	Land surface temperature
MC ratio	Measurement–calibration ratio
MetOp-A/B/C	Meteorological Operational satellite-A/B/C
MIKE SHE SWET	MIKE Système Hydrologique Européen Shuttleworth Wallace Evapotranspiration
MIRAS	Microwave Imaging Radiometer using Aperture Synthesis
MISDc	Italian: Modello Idrologico SemiDistribuito in continuo
MISDc-**2L**	MISDc two-layer
MODIS	Moderate resolution imaging spectroradiometer
MOPEX	Model Parameterization Experiment
MWRI	Microwave radiation imager
NASA	National Aeronautics and Space Administration
PDM	Probability distributed model
PF	Particle filter
PI	Polarization index
PSS	Peirce skill score
RFI	Radio frequency interferences
RMSE	Root mean square error
SAC model	Sacramento hydrologic model
SAC-D	Spanish: Satélite de Aplicaciones Científicas-D
SAC-SMA	Sacramento Soil Moisture Accounting Model
SAR	Synthetic aperture radar
SCAT	Scatterometer
SCRRM	Simplified continuous rainfall–runoff model
SCS-CN	Soil Conservation Service curve number
SI	Scattering index
SIM	French: Safran-Isba-Modcou
SM	Soil moisture
SMAP	Soil moisture active passive
SMMR	Scanning multichannel microwave radiometer
SMOS	Soil moisture and ocean salinity
SRTM	Shuttle Radar Topography Mission
SSM/I	Special sensor microwave/imager
SWAT	Soil and Water Assessment Tool
SWVI	Soil Wetness Variation Index

TC	Triple collocation
TMI	TRMM microwave imager
TRMM	Tropical Rainfall Measuring Mission
ubRMSE	Unbiased root mean square error
UNISDR	United Nations (UN) Office for Disaster Risk Reduction
UNOSAT	UN Institute for Training and Research's Operational Satellite Applications Programme
VI	Vegetation index
VIC model	Variable infiltration capacity model
VTCI	Vegetation temperature condition index
WCM	Water cloud model
XAJ model	Xin'anjiang model

References

1. Al-Yaari A, Wigneron JP, Dorigo W, Colliander A, Pellarin T, Hahn S, Mialon A, Richaume P, Fernandez-Moran R, Fan L, Kerr YH, De Lannoy G (2019) Assessment and inter-comparison of recently developed/reprocessed microwave satellite soil moisture products using ISMN ground-based measurements. Remote Sens Environ 224:289–303
2. Alcántara-Ayala I (2002) Geomorphology, natural hazards, vulnerability and prevention of natural disasters in developing countries. Geomorphology 47:107–124
3. Alexakis D, Mexis F-D, Vozinaki A-E, Daliakopoulos I, Tsanis I (2017) Soil moisture content estimation based on Sentinel-1 and auxiliary earth observation products. A hydrological approach. Sensors 17:1455
4. Alfieri L, Burek P, Dutra E, Krzeminski B, Muraro D, Thielen J, Pappenberger F (2013) GloFAS—global ensemble streamflow forecasting and flood early warning. Hydrol Earth Syst Sci 17: 1161–1175
5. Alvarez-Garreton C, Ryu D, Western AW, Crow WT, Robertson DE (2014) The impacts of assimilating satellite soil moisture into a rainfall-runoff model in a semi-arid catchment. J Hydrol 519: 2763–2774
6. Alvarez-Garreton C, Ryu D, Western AW, Su CH, Crow WT, Robertson DE, Leahy C (2015) Improving operational flood ensemble prediction by the assimilation of satellite soil moisture: comparison between lumped and semi-distributed schemes. Hydrol Earth Syst Sci 19:1659–1676
7. Alvarez-Garreton C, Ryu D, Western AW, Crow WT, Su CH, Robertson DR (2016) Dual assimilation of satellite soil moisture to improve streamflow prediction in data-scarce catchments. Water Resour Res 52:5357–5375
8. Attema E, Davidson M, Floury N, Levrini G, Rosich B, Rommen B, Snoeij P (2008) Sentinel-1 ESA's New European Radar Observatory. In: 7th European conference on synthetic aperture radar (pp. 1–4)
9. Attema E, Ulaby FT (1978) Vegetation modeled as a water cloud. Radio Sci 13:357–364
10. Bindlish R, Jackson T, Cosh M, Zhao T, Neill PO (2015) Global soil moisture from the Aquarius/SAC-D satellite: description and initial assessment. IEEE Geosci Remote Sens Lett 12:923–927
11. Bisselink B, van Meijgaard E, Dolman AJ, de Jeu RAM (2011) Initializing a regional climate model with satellite-derived soil moisture. J Geophys Res Atmos 116:D02121
12. Brakenridge GR, Cohen S, Kettner AJ, De Groeve T, Nghiem SV, Syvitski JPM, Fekete BM (2012) Calibration of satellite measurements of river discharge using a global hydrology model. J Hydrol 475:123–136
13. Brakenridge GR, Nghiem SV, Anderson E, Mic R (2007) Orbital microwave measurement of river discharge and ice status. Water Resour Res 43:W04405
14. Brocca L, Ciabatta L, Massari C, Moramarco T, Hahn S, Hasenauer S, Kidd R, Dorigo W, Wagner W, Levizzani V (2014) Soil as a natural rain gauge: estimating global rainfall from satellite soil moisture data. J Geophys Res Atmos 119: 2014JD021489
15. Brocca L, Melone F, Moramarco T, Wagner W, Naeimi V, Bartalis Z, Hasenauer S (2010) Improving runoff prediction through the assimilation of the ASCAT soil moisture product. Hydrol Earth Syst Sci 14:1881–1893
16. Brocca L, Moramarco T, Melone F, Wagner W, Hasenauer S, Hahn S (2012) Assimilation of surface- and root-zone ASCAT soil moisture products into rainfall–runoff modeling. IEEE Trans Geosci Remote Sens 50:2542–2555
17. Carsell K, Pingel N, Ford D (2004) Quantifying the benefit of a flood warning system. Nat Hazards Rev 5:131–140
18. Castillo V, Gomez-Plaza A, Martınez-Mena M (2003) The role of antecedent soil water content in the runoff response of semiarid catchments: a simulation approach. J Hydrol 284:114–130
19. Cenci L, Laiolo P, Gabellani S, Campo L, Silvestro F, Delogu F, Boni G, Rudari R (2016) Assimilation of H-SAF soil moisture products for flash flood early warning systems. Case study: Mediterranean catchments. IEEE J Sel Topics Appl Earth Observ Remote Sens 9:5634–5646
20. Chen F, Crow WT, Bindlish R, Colliander A, Burgin MS, Asanuma J, Aida K (2018) Global-scale evaluation of SMAP, SMOS and ASCAT soil moisture products using triple collocation. Remote Sens Environ 214:1–13
21. Chen F, Crow WT, Ryu D (2014) Dual forcing and state correction via soil moisture assimilation for improved rainfall–runoff modeling. J Hydrometeorol 15:1832–1848
22. Chen F, Crow WT, Starks PJ, Moriasi DN (2011) Improving hydrologic predictions of a catchment model via assimilation of surface soil moisture. Adv Water Resour 34:526–536
23. Choker M, Baghdadi N, Zribi M, El Hajj M, Paloscia S, Verhoest NE, Lievens H, Mattia F (2017) Evaluation of the Oh, Dubois and IEM backscatter models using a large dataset of SAR data and experimental soil measurements. Water 9:38
24. Chow VT, Maidment DR, Mays LW (1988) Applied hydrology. McGraw-Hill Series in Water Resources and Environmental Engineering. McGraw-Hill: New York. ISBN 0-07-010810-2. xiii, 572 pp. http://documentatiecentrum.watlab.be/imis.php?module=ref&refid=127685&basketaction=add
25. CRED/UNISDR (2016) Poverty and death: disaster mortality 1996–2015. United Nations Office for Disaster Risk Reduction,

and Centre for Research on the Epidemiology of Disasters, Brussels. https://www.unisdr.org/we/inform/publications/50589
26. Crow WT, Bindlish R, Jackson TJ (2005) The added value of spaceborne passive microwave soil moisture retrievals for forecasting rainfall-runoff partitioning. Geophys Res Lett 32(18). https://agupubs.onlinelibrary.wiley.com/doi/full/10.1029/2005GL023543
27. Crow WT, van Den Berg MJ, Huffman G, Pellarin T (2011) Correcting rainfall using satellite-based surface soil moisture retrievals: the Soil Moisture Analysis Rainfall Tool (SMART). Water Resour Res 47(8). https://agupubs.onlinelibrary.wiley.com/doi/full/10.1029/2011WR010576
28. Crow WT (2007) A novel method for quantifying value in spaceborne soil moisture retrievals. J Hydrometeorol 8:56–67
29. Crow WT, Berg AA, Cosh MH, Loew A, Mohanty BP, Panciera R, de Rosnay P, Ryu D, Walker JP (2012) Upscaling sparse ground-based soil moisture observations for the validation of coarse-resolution satellite soil moisture products. Rev Geophys 50:RG2002
30. Crow WT, Miralles DG, Cosh MH (2010) A quasi-global evaluation system for satellite-based surface soil moisture retrievals. IEEE Trans Geosci Remote Sens 48:2516–2527
31. Crow WT, Ryu D (2009) A new data assimilation approach for improving runoff prediction using remotely-sensed soil moisture retrievals. Hydrol Earth Syst Sci 13:1–16
32. Crow WT, Wood EF (2002) Impact of soil moisture aggregation on surface energy flux prediction during SGP'97. Geophys Res Lett 29:8-1–8-4
33. Crow WT, Zhan X (2007) Continental-scale evaluation of remotely sensed soil moisture products. IEEE Geosci Remote Sensi Lett 4:451–455
34. D'Odorico P, Caylor K, Okin GS, Scanlon TM (2007) On soil moisture–vegetation feedbacks and their possible effects on the dynamics of dryland ecosystems. J Geophys Res Biogeosci 112(G4). https://agupubs.onlinelibrary.wiley.com/doi/full/10.1029/2006JG000379
35. De Groeve T (2010) Flood monitoring and mapping using passive microwave remote sensing in Namibia. Geomat Nat Haz Risk 1:19–35
36. De Jeu RAM, Owe M (2003) Further validation of a new methodology for surface moisture and vegetation optical depth retrieval. Int J Remote Sens 24:4559–4578
37. De Jeu RAM, Wagner W, Holmes TRH, Dolman AJ, Giesen NC, Friesen J (2008) Global soil moisture patterns observed by space borne microwave radiometers and scatterometers. Surv Geophys 29:399–420
38. Dobson MC, Ulaby FT (1986) Active microwave soil moisture research. IEEE Trans Geosci Remote Sens(1):23–36. https://ieeexplore.ieee.org/abstract/document/407241
39. Dobson MC, Ulaby FT, Hallikainen MT, El-Rayes MA (1985) Microwave dielectric behavior of wet soil—part II: dielectric mixing models. IEEE Trans Geosci Remote Sens GE-23:12
40. Dong J, Crow WT, Duan Z, Wei L, Lu Y (2019) A double instrumental variable method for geophysical product error estimation. Remote Sens Environ 225:217–228
41. Dong J, Ni-Meister W, Houser PR (2007) Impacts of vegetation and cold season processes on soil moisture and climate relationships over Eurasia. J Geophys Res Atmos 112(D9). https://agupubs.onlinelibrary.wiley.com/doi/full/10.1029/2006JD007774
42. Dorigo W, Wagner W, Albergel C, Albrecht F, Balsamo G, Brocca L, Chung D, Ertl M, Forkel M, Gruber A, Haas E, Hamer PD, Hirschi M, Ikonen J, de Jeu R, Kidd R, Lahoz W, Liu YY, Miralles D, Mistelbauer T, Nicolai-Shaw N, Parinussa R, Pratola C, Reimer C, van der Schalie R, Seneviratne SI, Smolander T, Lecomte P (2017) ESA CCI Soil Moisture for improved Earth system understanding: state-of-the art and future directions. Remote Sens Environ 203:185–215
43. Dorigo WA, Gruber A, De Jeu RAM, Wagner W, Stacke T, Loew A, Albergel C, Brocca L, Chung D, Parinussa RM, Kidd R (2014) Evaluation of the ESA CCI soil moisture product using ground-based observations. Remote Sens Environ 162:380–395
44. Dorigo WA, Scipal K, Parinussa RM, Liu YY, Wagner W, de Jeu RAM, Naeimi V (2010) Error characterisation of global active and passive microwave soil moisture datasets. Hydrol Earth Syst Sci 14:2605–2616
45. Dorigo WA, Wagner W, Hohensinn R, Hahn S, Paulik C, Xaver A, Gruber A, Drusch M, Mecklenburg S, van Oevelen P, Robock A, Jackson T (2011) The International Soil Moisture Network: a data hosting facility for global in situ soil moisture measurements. Hydrol Earth Syst Sci 15:1675–1698
46. Dorigo WA, Xaver A, Vreugdenhil M, Gruber A, Hegyiová A, Sanchis-Dufau AD, Zamojski D, Cordes C, Wagner W, Drusch M (2013) Global automated quality control of in situ soil moisture data from the International Soil Moisture Network. Vadose Zone J 12(13). https://pubs.geoscienceworld.org/ssa/vzj/article/12/3/vzj2012.0097/91248
47. Draper C, Mahfouf J-F, Calvet J-C, Martin E, Wagner W (2011) Assimilation of ASCAT near-surface soil moisture into the SIM hydrological model over France. Hydrol Earth Syst Sci 15:3829–3841
48. Draper CS, Walker JP, Steinle PJ, De Jeu RAM, Holmes TRH (2009) An evaluation of AMSR–E derived soil moisture over Australia. Remote Sens Environ 113:703–710
49. Drusch M (2007) Initializing numerical weather prediction models with satellite-derived surface soil moisture: data assimilation experiments with ECMWF's Integrated Forecast System and the TMI soil moisture data set. J Geophys Res Atmos 112:D03102
50. Du J (2012) A method to improve satellite soil moisture retrievals based on Fourier analysis. Geophys Res Lett 39(15). https://agupubs.onlinelibrary.wiley.com/doi/full/10.1029/2012GL052435
51. Dubois PC, Van Zyl J, Engman T (1995) Measuring soil moisture with imaging radars. IEEE Trans Geosci Remote Sens 33:915–926
52. Durán-Barroso P, González J, Valdés JB (2016) Improvement of the integration of Soil Moisture Accounting into the NRCS-CN model. J Hydrol 542:809–819
53. Enenkel M, Reimer C, Dorigo W, Wagner W, Pfeil I, Parinussa R, De Jeu R (2016) Combining satellite observations to develop a global soil moisture product for near-real-time applications. Hydrol Earth Syst Sci 20:4191–4208
54. Engda TA, Kelleners TJ (2016) Soil moisture-based drought monitoring at different time scales: a case study for the U.S. Great Plains. JAWRA J Am Water Resour Assoc 52:77–88
55. Entekhabi D, Njoku EG, O'Neill PE, Kellogg KH, Crow WT, Edelstein WN, Entin JK, Goodman SD, Jackson TJ, Johnson J (2010a) The soil moisture active passive (SMAP) mission. Proc IEEE 98:704–716
56. Entekhabi D, Reichle RH, Koster RD, Crow WT (2010b) Performance metrics for soil moisture retrievals and application requirements. J Hydrometeorol 11:832–840
57. Famiglietti JS, Devereaux JA, Laymon CA, Tsegaye T, Houser PR, Jackson TJ, Graham ST, Rodell M, van Oevelen PJ (1999) Ground-based investigation of soil moisture variability within remote sensing footprints During the Southern Great Plains 1997 (SGP97) Hydrology Experiment. Water Resour Res 35:1839–1851
58. Fang B, Lakshmi V (2014) Soil moisture at watershed scale: remote sensing techniques. J Hydrol 516:258–272
59. Fang B, Lakshmi V, Bindlish R, Jackson TJ, Cosh M, Basara J (2013) Passive microwave soil moisture downscaling using

vegetation index and skin surface temperature. Vadose Zone J 12(3). https://dl.sciencesocieties.org/publications/vzj/abstracts/12/3/vzj2013.05.0089
60. Francois C, Quesney A, Ottlé C (2003) Sequential assimilation of ERS-1 SAR data into a coupled land surface–hydrological model using an extended Kalman filter. J Hydrometeorol 4:473–487
61. Fujii H, Koike T, Imaoka K (2009) Improvement of the AMSR-E algorithm for soil moisture estimation by introducing a fractional vegetation coverage dataset derived from MODIS data. J Remote Sens Soc Jpn 29:11
62. Fung AK, Li Z, Chen K-S (1992) Backscattering from a randomly rough dielectric surface. IEEE Trans Geosci Remote Sens 30:356–369
63. Geruo A, Velicogna I, Kimball JS, Du JY, Kim Y, Njoku E (2017) Satellite-observed changes in vegetation sensitivities to surface soil moisture and total water storage variations since the 2011 Texas drought. Environ Res Lett 12:054006
64. Gouweleeuw BT, van Dijk AIJM, Guerschman JP, Dyce P, Owe M (2012) Space-based passive microwave soil moisture retrievals and the correction for a dynamic open water fraction. Hydrol Earth Syst Sci 16:1635–1645
65. Gruber A, Dorigo WA, Crow W, Wagner W (2017) Triple collocation-based merging of satellite soil moisture retrievals. IEEE Trans Geosci Remote Sens 55:6780–6792
66. Gruber A, Su CH, Zwieback S, Crow W, Dorigo W, Wagner W (2016) Recent advances in (soil moisture) triple collocation analysis. Int J Appl Earth Obs Geoinf 45(Part B):200–211
67. Guha-Sapir D, Below R, Hoyois P (2015) EM-DAT: International Disaster Database. Université Catholique de Louvain, Brussels
68. Hain CR, Crow WT, Mecikalski JR, Anderson MC, Holmes T (2011) An intercomparison of available soil moisture estimates from thermal infrared and passive microwave remote sensing and land surface modeling. J Geophys Res Atmos 116:D15107
69. Hornacek M, Wagner W, Sabel D, Truong HL, Snoeij P, Hahmann T, Diedrich E, Doubkova M (2012) Potential for high resolution systematic global surface soil moisture retrieval via change detection using Sentinel-1. IEEE J Sel Topics Appl Earth Observ Remote Sens 5:1303–1311
70. Jackson TJ (1993) III. Measuring surface soil moisture using passive microwave remote sensing. Hydrol Process 7:139–152
71. Jacobs JM, Myers DA, Whitfield BM (2003) Improved rainfall/runoff estimates using remotely sensed soil moisture. JAWRA J Am Water Resour Assoc 39:313–324
72. Jin YQ (1999) A flooding index and its regional threshold value for monitoring floods in China from SSM/I data. Int J Remote Sens 20:1025–1030
73. Karthikeyan L, Pan M, Wanders N, Kumar DN, Wood EF (2017a) Four decades of microwave satellite soil moisture observations: part 1. A review of retrieval algorithms. Adv Water Resour 109:106–120
74. Karthikeyan L, Pan M, Wanders N, Kumar DN, Wood EF (2017b) Four decades of microwave satellite soil moisture observations: part 2. Product validation and inter-satellite comparisons. Adv Water Resour 109:236–252
75. Kerr YH, Waldteufel P, Wigneron J-P, Martinuzzi J, Font J, Berger M (2001) Soil moisture retrieval from space: the Soil Moisture and Ocean Salinity (SMOS) mission. IEEE Trans Geosci Remote Sens 39:1729–1735
76. Khan SI, Hong Y, Vergara HJ, Gourley JJ, Brakenridge GR, De Groeve T, Flamig ZL, Policelli F, Yong B (2012) Microwave satellite data for hydrologic modeling in ungauged basins. IEEE Geosci Remote Sens Lett 9:663–667
77. Kim G, Barros AP (2002) Downscaling of remotely sensed soil moisture with a modified fractal interpolation method using contraction mapping and ancillary data. Remote Sens Environ 83:400–413
78. Kim H, Parinussa R, Konings AG, Wagner W, Cosh MH, Lakshmi V, Zohaib M, Choi M (2018a) Global-scale assessment and combination of SMAP with ASCAT (active) and AMSR2 (passive) soil moisture products. Remote Sens Environ 204:260–275
79. Kim S, Balakrishnan K, Liu Y, Johnson F, Sharma A (2017) Spatial disaggregation of coarse soil moisture data by using high-resolution remotely sensed vegetation products. IEEE Geosci Remote Sens Lett 14:1604–1608
80. Kim S, Liu YY, Johnson FM, Parinussa RM, Sharma A (2015a) A global comparison of alternate AMSR2 soil moisture products: why do they differ? Remote Sens Environ 161:43–62
81. Kim S, Paik K, Johnson FM, Sharma A (2018b) Building a flood-warning framework for ungauged locations using low resolution, open-access remotely sensed surface soil moisture, precipitation, soil, and topographic information. IEEE J Sel Topics Appl Earth Observ Remote Sens 11:375–387
82. Kim S, Parinussa RM, Liu YY, Johnson FM, Sharma A (2015b) A framework for combining multiple soil moisture retrievals based on maximizing temporal correlation. Geophys Res Lett 42:6662–6670
83. Kim S, Sharma A (2019) The role of floodplain topography in deriving basin discharge using passive microwave remote sensing. Water Resour Res 55:1707–1716
84. Komma J, Blöschl G, Reszler C (2008) Soil moisture updating by Ensemble Kalman filtering in real-time flood forecasting. J Hydrol 357:228–242
85. Koren V, Moreda F, Smith M (2008) Use of soil moisture observations to improve parameter consistency in watershed calibration. Phys Chem Earth Parts A/B/C 33:1068–1080
86. Kornelsen KC, Coulibaly P (2015) Reducing multiplicative bias of satellite soil moisture retrievals. Remote Sens Environ 165:109–122
87. Koster RD, Brocca L, Crow WT, Burgin MS, De Lannoy GJ (2016) Precipitation estimation using L-band and C-band soil moisture retrievals. Water Resour Res 52:7213–7225
88. Koster RD, Suarez MJ (2001) Soil moisture memory in climate models. J Hydrometeorol 2:558–570
89. Lacava T, Cuomo V, Di Leo EV, Pergola N, Romano F, Tramutoli V (2005) Improving soil wetness variations monitoring from passive microwave satellite data: the case of April 2000 Hungary flood. Remote Sens Environ 96:135–148
90. Laiolo P, Gabellani S, Campo L, Silvestro F, Delogu F, Rudari R, Pulvirenti L, Boni G, Fascetti F, Pierdicca N (2016) Impact of different satellite soil moisture products on the predictions of a continuous distributed hydrological model. Int J Appl Earth Obs Geoinf 48:131–145
91. Lakshmi V, Fayne J, Bolten J (2018) A comparative study of available water in the major river basins of the world. J Hydrol 567:510–532. https://www.sciencedirect.com/science/article/pii/S002216941830800X
92. Li L, Njoku EG, Im E, Chang PS, Germain KS (2004) A preliminary survey of radio-frequency interference over the US in Aqua AMSR-E data. IEEE Trans Geosci Remote Sens 42:380–390
93. Li Y, Grimaldi S, Pauwels VR, Walker JP (2018) Hydrologic model calibration using remotely sensed soil moisture and discharge measurements: the impact on predictions at gauged and ungauged locations. J Hydrol 557:897–909
94. Li Y, Ryu D, Western AW, Wang Q, Robertson DE, Crow WT (2014) An integrated error parameter estimation and lag-aware data assimilation scheme for real-time flood forecasting. J Hydrol 519:2722–2736
95. Libertino A, Sharma A, Lakshmi V, Claps P (2016) A global assessment of the timing of extreme rainfall from TRMM and GPM for improving hydrologic design. Environ Res Lett 11:054003

96. Lievens H, De Lannoy G, Al Bitar A, Drusch M, Dumedah G, Franssen H-JH, Kerr Y, Tomer SK, Martens B, Merlin O (2016) Assimilation of SMOS soil moisture and brightness temperature products into a land surface model. Remote Sens Environ 180: 292–304
97. Lievens H, Tomer SK, Al Bitar A, De Lannoy GJ, Drusch M, Dumedah G, Franssen H-JH, Kerr Y, Martens B, Pan M (2015) SMOS soil moisture assimilation for improved hydrologic simulation in the Murray Darling Basin, Australia. Remote Sens Environ 168:146–162
98. Liu G (1998) A fast and accurate model for microwave radiance calculations. J Meteorol Soc Jpn 76:335–343
99. Liu YY, Parinussa RM, Dorigo WA, De Jeu RAM, Wagner W, van Dijk AIJM, McCabe MF, Evans JP (2011) Developing an improved soil moisture dataset by blending passive and active microwave satellite-based retrievals. Hydrol Earth Syst Sci 15:425–436
100. Loew A, Mauser W (2008) On the disaggregation of passive microwave soil moisture data using a priori knowledge of temporally persistent soil moisture fields. IEEE Trans Geosci Remote Sens 46:819–834
101. Loew A, Schlenz F (2011) A dynamic approach for evaluating coarse scale satellite soil moisture products. Hydrol Earth Syst Sci 15:75–90
102. López PL, Sutanudjaja EH, Schellekens J, Sterk G, Bierkens MF (2017) Calibration of a large-scale hydrological model using satellite-based soil moisture and evapotranspiration products. Hydrol Earth Syst Sci 21:3125–3144
103. Massari C, Brocca L, Barbetta S, Papathanasiou C, Mimikou M, Moramarco T (2014a) Using globally available soil moisture indicators for flood modelling in Mediterranean catchments. Hydrol Earth Syst Sci 18:839
104. Massari C, Brocca L, Moramarco T, Tramblay Y, Didon Lescot J-F (2014b) Potential of soil moisture observations in flood modelling: estimating initial conditions and correcting rainfall. Adv Water Resour 74:44–53
105. Massari C, Brocca L, Tarpanelli A, Moramarco T (2015) Data assimilation of satellite soil moisture into rainfall-runoff modelling: a complex recipe? Remote Sens 7:11403–11433
106. Matgen P, Fenicia F, Heitz S, Plaza D, de Keyser R, Pauwels VR, Wagner W, Savenije H (2012) Can ASCAT-derived soil wetness indices reduce predictive uncertainty in well-gauged areas? A comparison with in situ observed soil moisture in an assimilation application. Adv Water Resour 44:49–65
107. May W, Meier A, Rummukainen M, Berg A, Chéruy F, Hagemann S (2015) Contributions of soil moisture interactions to climate change in the tropics in the GLACE–CMIP5 experiment. Clim Dyn 45:1–23
108. McColl KA, Vogelzang J, Konings AG, Entekhabi D, Piles M, Stoffelen A (2014) Extended triple collocation: estimating errors and correlation coefficients with respect to an unknown target. Geophys Res Lett 41:6229–6236
109. Meng S, Xie X, Liang S (2017) Assimilation of soil moisture and streamflow observations to improve flood forecasting with considering runoff routing lags. J Hydrol 550:568–579
110. Merlin O, Walker JP, Chehbouni A, Kerr Y (2008) Towards deterministic downscaling of SMOS soil moisture using MODIS derived soil evaporative efficiency. Remote Sens Environ 112: 3935–3946
111. Mo T, Choudhury B, Schmugge T, Wang J, Jackson T (1982) A model for microwave emission from vegetation-covered fields. J Geophys Res Oceans 87:11229–11237
112. Mo T, Schmugge TJ, Jackson TJ (1984) Calculations of radar backscattering coefficient of vegetation-covered soils. Remote Sens Environ 15:119–133
113. Moran MS, Hymer DC, Qi J, Sano EE (2000) Soil moisture evaluation using multi-temporal synthetic aperture radar (SAR) in semiarid rangeland. Agric For Meteorol 105:69–80
114. Naeimi V, Scipal K, Bartalis Z, Hasenauer S, Wagner W (2009) An improved soil moisture retrieval algorithm for ERS and METOP scatterometer observations. IEEE Trans Geosci Remote Sens 47:1999–2013
115. Narayan U, Lakshmi V, Njoku EG (2004) A simple algorithm for spatial disaggregation of radiometer derived soil moisture using higher resolution radar observations. In, IGARSS 2004. 2004 IEEE International Geoscience and Remote Sensing Symposium 3:1877–1879. IEEE. https://ieeexplore.ieee.org/abstract/document/1370706
116. Njoku EG, Ashcroft P, Chan TK, Li L (2005) Global survey and statistics of radio-frequency interference in AMSR-E land observations. IEEE Trans Geosci Remote Sens 43:938–947
117. Njoku EG, Entekhabi D (1996) Passive microwave remote sensing of soil moisture. J Hydrol 184:101–129
118. Njoku EG, Kong J-A (1977) Theory for passive microwave remote sensing of near-surface soil moisture. J Geophys Res 82: 3108–3118
119. Norbiato D, Borga M, Degli Esposti S, Gaume E, Anquetin S (2008) Flash flood warning based on rainfall thresholds and soil moisture conditions: an assessment for gauged and ungauged basins. J Hydrol 362:274–290
120. Oh Y, Sarabandi K, Ulaby FT (1992) An empirical model and an inversion technique for radar scattering from bare soil surfaces. IEEE Trans Geosci Remote Sens 30:370–381
121. Owe M, De Jeu RAM, Holmes T (2008) Multisensor historical climatology of satellite-derived global land surface moisture. J Geophys Res Earth Surf 113:F01002
122. Paloscia S, Pettinato S, Santi E, Notarnicola C, Pasolli L, Reppucci A (2013) Soil moisture mapping using Sentinel-1 images: algorithm and preliminary validation. Remote Sens Environ 134:234–248
123. Panciera R, Tanase MA, Lowell K, Walker JP (2014) Evaluation of IEM, Dubois, and Oh radar backscatter models using airborne L-band SAR. IEEE Trans Geosci Remote Sens 52:4966–4979
124. Papa F, Prigent C, Rossow WB (2008) Monitoring flood and discharge variations in the large Siberian rivers from a multi-satellite technique. Surv Geophys 29:297–317
125. Parajka J, Naeimi V, Blöschl G, Komma J (2009) Matching ERS scatterometer based soil moisture patterns with simulations of a conceptual dual layer hydrologic model over Austria. Hydrol Earth Syst Sci 13:259–271
126. Parinussa R, de Jeu R, van der Schalie R, Crow W, Lei F, Holmes T (2016) A quasi-global approach to improve day-time satellite surface soil moisture anomalies through the land surface temperature input. Climate 4:50
127. Parinussa RM, Holmes TRH, Crow WT (2011a) The impact of land surface temperature on soil moisture anomaly detection from passive microwave observations. Hydrol Earth Syst Sci Discuss 8: 3135–3151
128. Parinussa RM, Holmes TRH, Wanders N, Dorigo WA, de Jeu RAM (2014a) A preliminary study toward consistent soil moisture from AMSR2. J Hydrometeorol 16:932–947
129. Parinussa RM, Meesters AGCA, Liu Y, Dorigo W, Wagner W, De Jeu RAM (2011b) Error estimates for near-real-time satellite soil moisture as derived from the land parameter retrieval model. IEEE Geosci Remote Sensi Lett 8:779–783
130. Parinussa RM, Wang G, Holmes TRH, Liu YY, Dolman AJ, de Jeu RAM, Jiang T, Zhang P, Shi J (2014b) Global surface soil moisture from the Microwave Radiation Imager onboard the Fengyun-3B satellite. Int J Remote Sens 35:7007–7029

131. Pathiraja S, Westra S, Sharma A (2012) Why continuous simulation? The role of antecedent moisture in design flood estimation. Water Resour Res 48:W06534
132. Paulik C, Dorigo W, Wagner W, Kidd R (2014) Validation of the ASCAT Soil Water Index using in situ data from the International Soil Moisture Network. Int J Appl Earth Obs Geoinf 30:1–8
133. Pellarin T, Louvet S, Gruhier C, Quantin G, Legout C (2013) A simple and effective method for correcting soil moisture and precipitation estimates using AMSR-E measurements. Remote Sens Environ 136:28–36
134. Pellenq J, Kalma J, Boulet G, Saulnier GM, Wooldridge S, Kerr Y, Chehbouni A (2003) A disaggregation scheme for soil moisture based on topography and soil depth. J Hydrol 276:112–127
135. Peng J, Loew A, Merlin O, Verhoest NEC (2017) A review of spatial downscaling of satellite remotely sensed soil moisture. Rev Geophys 55:341–366
136. Peng J, Niesel J, Loew A (2015) Evaluation of soil moisture downscaling using a simple thermal-based proxy—the REMEDHUS network (Spain) example. Hydrol Earth Syst Sci 19:4765
137. Petropoulos GP, Ireland G, Barrett B (2015) Surface soil moisture retrievals from remote sensing: current status, products & future trends. Phys Chem Earth Parts A/B/C 83-84:36–56
138. Pham H, Do C, Renzullo L (2017) Assimilating stream flow, evapotranspiration and soil moisture data in AWRA-L model with particle filter. In, 22nd International Congress on Modelling and Simulation. https://www.mssanz.org.au/modsim2017/H5/pham.pdf
139. Piepmeier JR, Johnson JT, Mohammed PN, Bradley D, Ruf C, Aksoy M, Garcia R, Hudson D, Miles L, Wong M (2014) Radio-frequency interference mitigation for the soil moisture active passive microwave radiometer. IEEE Trans Geosci Remote Sens 52:761–775
140. Piles M, Camps A, Vall-Llossera M, Corbella I, Panciera R, Rudiger C, Kerr YH, Walker J (2011) Downscaling SMOS-derived soil moisture using MODIS visible/infrared data. IEEE Trans Geosci Remote Sens 49:3156–3166
141. Prevot L, Dechambre M, Taconet O, Vidal-Madjar D, Normand M, Gallej S (1993) Estimating the characteristics of vegetation canopies with airborne radar measurements. Int J Remote Sens 14:2803–2818
142. Rajib MA, Merwade V, Yu Z (2016) Multi-objective calibration of a hydrologic model using spatially distributed remotely sensed/in-situ soil moisture. J Hydrol 536:192–207
143. Rao YS, Sharma S (2006) Monitoring of flood over Gujarat region using AQUA AMSR-E derived surface soil moisture. In Disaster Forewarning Diagnostic Methods and Management. International Society for Optics and Photonics 6412:641208. https://www.spiedigitallibrary.org/conference-proceedings-of-spie/6412/641208/Monitoring-of-flood-over-Gujarat-region-using-AQUA-AMSR-E/10.1117/12.697525.full?SSO=1
144. Rautiainen K, Lemmetyinen J, Schwank M, Kontu A, Ménard CB, Mätzler C, Drusch M, Wiesmann A, Ikonen J, Pulliainen J (2014) Detection of soil freezing from L-band passive microwave observations. Remote Sens Environ 147:206–218
145. Reichle RH, Koster RD (2004) Bias reduction in short records of satellite soil moisture. Geophys Res Lett 31:L19501
146. Revilla-Romero B, Thielen J, Salamon P, De Groeve T, Brakenridge GR (2014) Evaluation of the satellite-based Global Flood Detection System for measuring river discharge: influence of local factors. Hydrol Earth Syst Sci 18:4467–4484
147. Ridler ME, Madsen H, Stisen S, Bircher S, Fensholt R (2014) Assimilation of SMOS-derived soil moisture in a fully integrated hydrological and soil-vegetation-atmosphere transfer model in Western Denmark. Water Resour Res 50:8962–8981
148. Román-Cascón C, Pellarin T, Gibon F, Brocca L, Cosme E, Crow W, Fernández-Prieto D, Kerr YH, Massari C (2017) Correcting satellite-based precipitation products through SMOS soil moisture data assimilation in two land-surface models of different complexity: API and SURFEX. Remote Sens Environ 200:295–310
149. Ruggenthaler R, Schöberl F, Markart G, Klebinder K, Hammerle A, Leitinger G (2015) Quantification of soil moisture effects on runoff formation at the hillslope scale. J Irrig Drain Eng 141:05015001
150. Sabaghy S, Walker JP, Renzullo LJ, Jackson TJ (2018) Spatially enhanced passive microwave derived soil moisture: capabilities and opportunities. Remote Sens Environ 209:551–580
151. Schmugge T, Neill PEO, Wang JR (1986) Passive microwave soil moisture research. IEEE Trans Geosci Remote Sens GE-24:12–22
152. Schmugge TJ (1980) Effect of texture on microwave emission from soils. IEEE Trans Geosci Remote Sens GE-18:353–361
153. Scipal K, Holmes T, de Jeu R, Naeimi V, Wagner W (2008) A possible solution for the problem of estimating the error structure of global soil moisture data sets. Geophys Res Lett 35:L24403
154. Silvestro F, Gabellani S, Rudari R, Delogu F, Laiolo P, Boni G (2015) Uncertainty reduction and parameter estimation of a distributed hydrological model with ground and remote-sensing data. Hydrol Earth Syst Sci 19:1727–1751
155. Sohrabi M, Ryu J, Abatzoglou J, Tracy J (2015) Development of soil moisture drought index to characterize droughts. J Hydrol Eng 0:04015025
156. Stoffelen A (1998) Toward the true near-surface wind speed: Error modeling and calibration using triple collocation. J Geophys Res Oceans (1978–2012) 103:7755–7766
157. Su C-H, Narsey SY, Gruber A, Xaver A, Chung D, Ryu D, Wagner W (2015) Evaluation of post-retrieval de-noising of active and passive microwave satellite soil moisture. Remote Sens Environ 163:127–139
158. Su C-H, Ryu D, Crow WT, Western AW (2014) Beyond triple collocation: applications to soil moisture monitoring. J Geophys Res Atmos 119:2013JD021043
159. Su C-H, Ryu D, Western AW, Wagner W (2013) De-noising of passive and active microwave satellite soil moisture time series. Geophys Res Lett 40:3624–3630
160. Su CH, Ryu D (2015) Multi-scale analysis of bias correction of soil moisture. Hydrol Earth Syst Sci 19:17–31
161. Sutanudjaja E, Van Beek L, De Jong S, Van Geer F, Bierkens M (2014) Calibrating a large-extent high-resolution coupled groundwater-land surface model using soil moisture and discharge data. Water Resour Res 50:687–705
162. Syvitski JP, Brakenridge GR (2013) Causation and avoidance of catastrophic flooding along the Indus River, Pakistan. GSA Today 23:4–10
163. Temimi M, Leconte R, Chaouch N, Sukumal P, Khanbilvardi R, Brissette F (2010) A combination of remote sensing data and topographic attributes for the spatial and temporal monitoring of soil wetness. J Hydrol 388:28–40
164. Tomer S, Al Bitar A, Sekhar M, Zribi M, Bandyopadhyay S, Kerr Y (2016) MAPSM: a spatio-temporal algorithm for merging soil moisture from active and passive microwave remote sensing. Remote Sens 8:990
165. Torres R, Snoeij P, Geudtner D, Bibby D, Davidson M, Attema E, Potin P, Rommen B, Floury N, Brown M (2012) GMES Sentinel-1 mission. Remote Sens Environ 120:9–24
166. Ulaby FT, Dubois PC, Van Zyl J (1996) Radar mapping of surface soil moisture. J Hydrol 184:57–84
167. Ulaby FT, Long DG, Blackwell WJ, Elachi C, Fung AK, Ruf C, Van Zyl J (2014) Microwave Radar and Radiometric Remote Sensing: University of Michigan Press. https://books.google.com.au/books?id=y6pZngEACAAJ&dq=microwave+radar+

and+radiometric+remote+sensing&hl=en&sa=X&ved=0ahUKEwim8rqVzNblAhUDfisKHUn7B-wQ6AEIKTAA
168. Vernieuwe H, De Baets B, Minet J, Pauwels VRN, Lambot S, Vanclooster M, Verhoest NEC (2011) Integrating coarse-scale uncertain soil moisture data into a fine-scale hydrological modelling scenario. Hydrol Earth Syst Sci 15:3101–3114
169. Wagner W, Hahn S, Kidd R, Melzer T, Bartalis Z, Hasenauer S, Figa-Saldaña J, de Rosnay P, Jann A, Schneider S (2013) The ASCAT soil moisture product: a review of its specifications, validation results, and emerging applications. Meteorol Z 22:5–33
170. Wagner W, Lemoine G, Rott H (1999) A method for estimating soil moisture from ERS scatterometer and soil data. Remote Sens Environ 70:191–207
171. Wagner W, Scipal K, Pathe C, Gerten D, Lucht W, Rudolf B (2003) Evaluation of the agreement between the first global remotely sensed soil moisture data with model and precipitation data. J Geophys Res Atmos 108:4611
172. Walker J, Panciera R, Monerris A (2013) A national soil moisture monitoring capability, Annex 12. Basis of an Australian radar soil moisture algorithm theoretical baseline document. Retrieved from Australian Centre for Space Engineering Research (ACSER), Faculty of Engineering, University of New South Wales, Sydney, Australia http://www.garada.unsw.edu.au/Final%20Report/Annex%2012.%20Basis%20Of%20An%20Australian%20Radar%20Soil%20Moisture%20Algorithm%20Theoretical%20Baseline%20Document.pdf
173. Walker JP, Houser PR (2004) Requirements of a global near-surface soil moisture satellite mission: accuracy, repeat time, and spatial resolution. Adv Water Resour 27:785–801
174. Wan Z, Wang P, Li X (2004) Using MODIS Land Surface Temperature and Normalized Difference Vegetation Index products for monitoring drought in the southern Great Plains, USA. Int J Remote Sens 25:61–72
175. Wanders N, Bierkens MFP, de Jong SM, de Roo A, Karssenberg D (2014a) The benefits of using remotely sensed soil moisture in parameter identification of large-scale hydrological models. Water Resour Res 50:6874–6891
176. Wanders N, Karssenberg D, de Roo A, de Jong SM, Bierkens MFP (2014b) The suitability of remotely sensed soil moisture for improving operational flood forecasting. Hydrol Earth Syst Sci 18:2343–2357
177. Wang JR, Choudhury BJ (1981) Remote sensing of soil moisture content, over bare field at 1.4 GHz frequency. J Geophys Res Oceans 86:5277–5282
178. Wang JR, Schmugge TJ (1980) An empirical model for the complex dielectric permittivity of soils as a function of water content. IEEE Trans Geosci Remote Sens GE-18:288–295
179. Wigneron J, Schmugge TJ, Chanzy A, Calvet J, Kerr Y (1998) Use of passive microwave remote sensing to monitor soil moisture. Agronomie 18:27–43
180. Wilheit TT (1978) Radiative transfer in a plane stratified dielectric. IEEE Trans Geosci Electron 16:138–143
181. Wilks DS (2011) Statistical methods in the atmospheric sciences (Vol. 100). Academic press. https://books.google.com.au/books?id=IJuCVtQ0ySIC&dq=Statistical+methods+in+the+atmospheric+sciences&lr=&source=gbs_navlinks_s
182. Wright AJ, Walker JP, Pauwels VR (2018) Identification of hydrologic models, optimized parameters, and rainfall inputs consistent with in situ streamflow and rainfall and remotely sensed soil moisture. J Hydrometeorol 19:1305–1320
183. Wu Q, Liu H, Wang L, Deng C (2016) Evaluation of AMSR2 soil moisture products over the contiguous United States using in situ data from the International Soil Moisture Network. Int J Appl Earth Obs Geoinf 45:187–199
184. Yee MS, Walker JP, Monerris A, Rüdiger C, Jackson TJ (2016) On the identification of representative in situ soil moisture monitoring stations for the validation of SMAP soil moisture products in Australia. J Hydrol 537:367–381
185. Yilmaz MT, Crow WT (2013) The optimality of potential rescaling approaches in land data assimilation. J Hydrometeorol 14:650–660
186. Yilmaz MT, Crow WT (2014) Evaluation of assumptions in soil moisture triple collocation analysis. J Hydrometeorol 15:1293–1302
187. Zhan W, Pan M, Wanders N, Wood E (2015) Correction of real-time satellite precipitation with satellite soil moisture observations. Hydrol Earth Syst Sci 19:4275–4291
188. Zhang R, Kim S, Sharma A (2019) A comprehensive validation of the SMAP Enhanced Level-3 Soil Moisture product using ground measurements over varied climates and landscapes. Remote Sens Environ 223:82–94
189. Zhou W-C, Han Z, Han S-Y, Wang Y-Q, Zhang X-W, Wu Y-S (2019) Characteristics of L-band radio frequency interference detected via the soil moisture active passive radiometer in China and its offshore areas. Results Phys 12:1859–1865
190. Zwieback S, Dorigo W, Wagner W (2013) Estimation of the temporal autocorrelation structure by the collocation technique with an emphasis on soil moisture studies. Hydrol Sci J 58:1729–1747